

THEORY OF INTERSTELLAR SHOCKS

Bruce T. Draine

Princeton University Observatory, Peyton Hall, Princeton,
New Jersey 08544

Christopher F. McKee

Departments of Physics and Astronomy, University of California,
Berkeley, California 94720

KEY WORDS: interstellar medium, shock waves

1. INTRODUCTION

The interstellar medium is intermittently disturbed by violent events—supernova explosions being but one example—which cause large increases in the local pressure. As the result of the pressure increase, the disturbed region will expand. If the pressure increase exceeds a minimum value, a “shock front” will develop at the leading edge of this expanding disturbance, and the flow in the neighborhood of this front is referred to as a “shock” or “shock wave.” Besides supernova explosions, interstellar shock waves may be driven by the pressure of photoionized gas, stellar winds, and collisions between fast-moving clumps of interstellar gas.

A shock wave is an *irreversible, pressure-driven* fluid-dynamical disturbance. The irreversible character is due to entropy generation as ordered kinetic energy is dissipated into heat. In neutral gas, the dissipation is due to molecular viscosity in the shock transition (where large velocity gradients and viscous stresses are present). In low-density plasmas, the dissipation may be collisionless, and due to collective motions of the charged particles and the resulting electromagnetic fields. In partially-ionized gases, the dissipation may sometimes be primarily due to “friction”

associated with neutral-ion “slip.” Regardless of the dissipative process, shock waves are always compressive. As we shall see, however, the structure of the shock transition, and the emission from the hot shocked gas, may be quite sensitive to the dissipational mechanism.

We will be interested primarily in understanding shocks in the idealized limit where they are steady, so that a reference frame can be adopted in which the flow is stationary (i.e. $\partial/\partial t = 0$). Further simplification is possible if the flow is idealized as plane-parallel ($\partial/\partial y = \partial/\partial z = 0$). The fluid-dynamical structure of a steady, plane-parallel shock is illustrated in Figure 1. The preshock gas, approaching from the left (in the “shock frame”) is irradiated by photons emitted from the hot, shocked gas on the other side of the shock. This radiation may heat and ionize the preshock gas; this preheated and pre-ionized zone is referred to as the “radiative precursor.” The preshock gas undergoes very little deceleration until it reaches the “shock transition” where the bulk of the energy dissipation (and entropy generation) occurs. As it flows through the shock transition it is com-

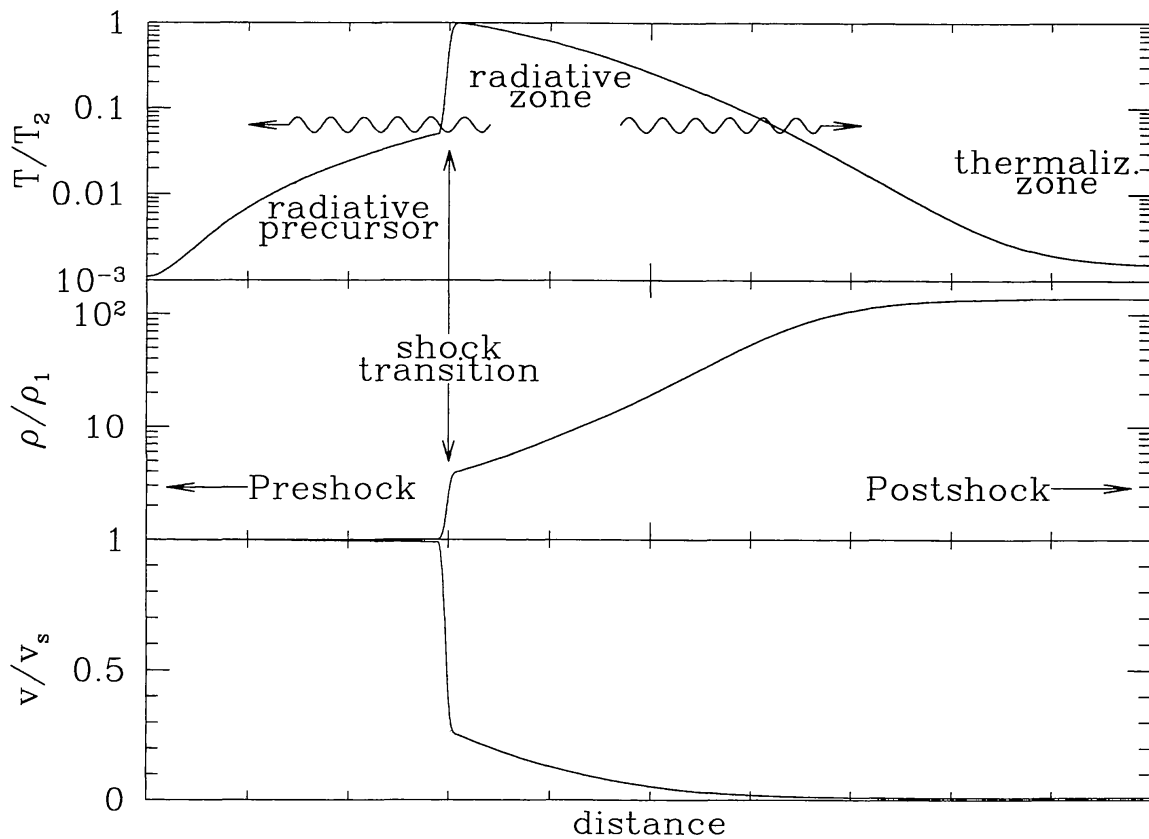


Figure 1 Schematic structure of a strong (single-fluid) shock wave showing temperature T , density ρ , and velocity v (relative to the shock front). ρ_1 is the preshock density, and T_2 is the temperature just behind the shock transition.

pressed by a factor ~ 4 , and its flow velocity (in the “shock frame”) is reduced by the same factor. The decrease in ordered kinetic energy is accompanied by an increase in thermal energy. The hot postshock gas radiates its energy as it flows away from the shock transition; as it cools it is further compressed, since the postshock region is at approximately constant pressure. The region within which the bulk of the radiative losses occurs is designated the “radiative” zone. The radiated energy which propagates toward the preshock gas is responsible for the “radiative precursor”; a fraction of the photons which propagate in the downstream direction are absorbed by the gas (and perhaps dust) far downstream and contribute to the heating of this gas which has attained near-equilibrium between heating and cooling (the “thermalization zone”).

We seek here to outline the physical principles underlying our theoretical understanding of the structure of interstellar shock waves; we try to make clear where our theoretical analyses are thought to be secure, as well as to identify the areas in which existing theory appears to be incomplete. We do *not* aim to discuss the role of shock waves in the global dynamics of the interstellar medium, nor do we attempt to mention all the different astrophysical scenarios in which interstellar shock waves may appear. The literature on observations of shocked interstellar gas is now so vast that we do not attempt to review it; we refer to observations only where they bear immediately on the theoretical issues we discuss. In order to provide a self-contained review article, we perform overlap with previous reviews (McKee & Hollenbach 1980, Shull & Draine 1987, McKee & Draine 1991). For an extensive discussion of the physics of shock waves with an emphasis on laboratory plasmas, the reader is referred to the monograph by Liberman & Velikovich (1986).

2. SINGLE FLUID SHOCKS

In this section we review the fluid dynamics of single fluid shocks. By “single fluid” (as opposed to “multifluid”) we refer to flows where all components (e.g. atoms, ions, and electrons) may be approximated as having a common flow velocity v . Subsections 2.1 (Fluid Equations) and 2.2 (Jump Conditions) are somewhat technical; the reader seeking only an overview may wish to skip directly to subsection 2.3.

2.1 *Fluid Equations*

The fluid motion is dictated by the conservation of mass, momentum, and energy (e.g. Landau & Lifshitz 1959), together with Maxwell’s equations.

In the case of a single fluid, the laws of mass, momentum, and energy conservation become (Tidman & Krall 1971, Hollenbach & McKee 1979):

$$\frac{\partial \rho}{\partial t} + \frac{\partial}{\partial x_k} (\rho v_k) = 0, \quad (2.1)$$

$$\frac{\partial}{\partial t} (\rho v_j) + \frac{\partial}{\partial x_k} \left(\rho v_j v_k + P \delta_{jk} - \sigma_{jk} + \frac{B^2}{8\pi} \delta_{jk} - \frac{1}{4\pi} B_j B_k \right) = 0, \quad (2.2)$$

$$\frac{\partial}{\partial t} u + \frac{\partial}{\partial x_k} (u v_k + q_k) + (P \delta_{jk} - \sigma_{jk}) \frac{\partial v_j}{\partial x_k} + \frac{\partial F_k}{\partial x_k} = 0, \quad (2.3)$$

where ρ , \mathbf{v} , and P are the density, velocity, and pressure; \mathbf{B} is the magnetic field, u is the fluid energy density [$u = (3/2)P + u_{\text{int}}$, where u_{int} is the “internal” energy density], \mathbf{q} is the heat flux due to thermal conduction, \mathbf{F} is the radiative flux, and σ_{jk} is the viscous stress tensor. The electrical conductivity of the fluid is assumed to be infinite, so that the fluid is everywhere electrically neutral. Summation over repeated indices is implied. The divergence of the radiative flux is $\nabla \cdot \mathbf{F} = \Lambda$, where Λ is the net rate per volume of energy removal due to radiative cooling and heating. One may eliminate u_{int} from Equation (2.3) by defining an “effective” loss function

$$\Lambda_{\text{eff}} \equiv \Lambda + (\partial/\partial x_k) (u_{\text{int}} v_k) + (\partial/\partial t) u_{\text{int}}; \quad (2.4)$$

Λ_{eff} then includes energy “losses” associated with, e.g. ionization or dissociation, and the energy conservation equation becomes

$$\frac{\partial}{\partial t} \left(\frac{3}{2} P \right) + \frac{\partial}{\partial x_k} \left(\frac{3}{2} P v_k + q_k \right) + (P \delta_{jk} - \sigma_{jk}) \frac{\partial v_j}{\partial x_k} + \Lambda_{\text{eff}} = 0. \quad (2.5)$$

Some flows may contain plasma waves with periods short compared to flow times of interest. We may then take the flow variables ρ , \mathbf{v} , \mathbf{B} , u , and P to be averaged over the waves in the plasma. In this case (2.2) neglects the momentum flux which may be associated with the short period waves (see Dewar 1970).

If we assume the electric field in the fluid frame to vanish, then $\mathbf{E} + (1/c)\mathbf{v} \times \mathbf{B} = 0$, and the magnetic field is determined by

$$\frac{\partial}{\partial t} B_j + \frac{\partial}{\partial x_k} (v_k B_j - v_j B_k) = 0. \quad (2.6)$$

This equation also applies to \mathbf{B} after averaging over waves with periods that are short compared to the characteristic flow time scale. From (2.2–2.6) we may obtain an alternate form of the energy equation:

$$\frac{\partial}{\partial t} \left(\frac{1}{2} \rho v^2 + u + \frac{B^2}{8\pi} \right) + \frac{\partial}{\partial x_k} \times \left[\left(\frac{1}{2} \rho v^2 + u + P + \frac{B^2}{4\pi} \right) v_k - \sigma_{kj} v_j - \frac{B_j B_k}{4\pi} v_j + F_k \right] = 0. \quad (2.7)$$

These equations are restricted to flows where all plasma components have a common flow velocity \mathbf{v} , although different components (e.g. ions and electrons) may have different temperatures or even anisotropic velocity distributions ($\sigma_{jk} \neq 0$).

2.2 Jump Conditions

If we assume that a shock “front” is present which is locally plane-parallel and steady (i.e. the time scale for variation is long compared to the time required to flow across the front) then we may integrate Equations 2.1, 2.2, 2.6, and 2.7 across the shock front to obtain “jump conditions.” We will assume that the viscous stress and conductive heat flux are negligible on either side of the shock front. Letting the “parallel” direction be the direction along the normal to the shock front, the jump conditions are

$$[\rho v_{\parallel}] = 0, \quad (2.8)$$

$$[B_{\parallel}] = 0, \quad (2.9)$$

$$[v_{\parallel} \mathbf{B}_{\perp} - B_{\parallel} \mathbf{v}_{\perp}] = 0, \quad (2.10)$$

$$\left[\rho v_{\parallel}^2 + P + \frac{1}{8\pi} B_{\perp}^2 \right] = 0, \quad (2.11)$$

$$\left[\rho v_{\parallel} \mathbf{v}_{\perp} - \frac{1}{4\pi} B_{\parallel} \mathbf{B}_{\perp} \right] = 0, \quad (2.12)$$

$$\left[v_{\parallel} \left(\frac{1}{2} \rho v^2 + P + u \right) + \frac{1}{4\pi} (B_{\perp}^2 v_{\parallel} - B_{\parallel} \mathbf{B}_{\perp} \cdot \mathbf{v}_{\perp}) + F_{\parallel} \right] = 0. \quad (2.13)$$

The notation $[f] \equiv f(x_2) - f(x_1)$, where subscripts 1 and 2 denote points upstream and downstream of the shock transition; the viscous stresses σ_{jk} are assumed to be negligible at these positions. These jump conditions must be supplemented by an equation determining the internal energy $u_{\text{int}} = u - 3P/2$ and equations describing possible compositional changes. In some cases it is possible to take the internal energy to be proportional to the pressure: $u = P/(\gamma - 1)$, where γ is the so-called adiabatic index. We assume that γ is constant across the shock.

Before proceeding, recall that an MHD fluid supports three wave modes: the “slow,” “intermediate,” and “fast” waves, with propagation speeds $u_s < u_i < u_f$ given by (Priest 1982)

$$\left. \begin{array}{l} u_f \\ u_s \end{array} \right\} = 2^{-1/2} [(v_A^2 + c_s^2) \pm (v_A^4 + c_s^4 - 2v_A^2 c_s^2 \cos 2\theta)^{1/2}]^{1/2}, \quad (2.14)$$

$$u_i = v_A \cos \theta, \quad (2.15)$$

$$v_A \equiv B/(4\pi\rho)^{1/2}, \quad (2.16)$$

$$c_s \equiv (\gamma P/\rho)^{1/2}, \quad (2.17)$$

where v_A and c_s are the Alfvén and sound speeds, and θ is the angle between the direction of propagation and \mathbf{B} . The fast and slow modes are compressive; they change the magnitude of the field, but not its plane of polarization. The intermediate mode is noncompressive; it can change the plane of polarization of the field, but not its magnitude.

To elucidate the nature of these modes and the shocks associated with them, one can combine Equations (2.8)–(2.10) and (2.12) to find

$$\left[\left(\frac{v_{\parallel}^2}{u_i^2} - 1 \right) \mathbf{B}_{\perp} \right] = 0. \quad (2.18)$$

This shows that only intermediate waves ($v_{\parallel} = u_i$), not shocks, can cause \mathbf{B}_{\perp} to move out of its original plane. Shocks are coplanar: The plane defined by \mathbf{B} and the shock normal is invariant across the shock. A second consequence of Equation (2.18) is that the sign of \mathbf{B}_{\perp} changes across the shock if and only if the shock makes a transition from super-intermediate flow ($v_{\parallel 1} > u_{i1}$) to sub-intermediate flow ($v_{\parallel 2} < u_{i2}$).

MHD shocks cause the flow velocity to jump from above the phase velocity of a given wave to below. Following Kennel et al (1990), we classify the flow state in order of decreasing velocity as type 1 if $u_f < v_{\parallel}$; type 2 if $u_i < v_{\parallel} < u_f$; type 3 if $u_s < v_{\parallel} < u_i$; and type 4 if $v_{\parallel} < u_s$. There are 6 distinct types of MHD shocks: fast shocks (type 1 → 2), slow shocks (3 → 4), and 4 intermediate shocks (1 → 3, 2 → 3, 1 → 4, and 2 → 4). Let $v_s = v_{\parallel 1}$ be the shock velocity measured along the shock normal. Fast shocks have $v_s > u_{f1}$; the flow is super-intermediate on both sides, and the magnetic field increases in magnitude but does not reverse direction. Slow shocks are sub-intermediate on both sides; the magnetic field decreases in magnitude but does not reverse direction. Intermediate shocks cause a transition from super-intermediate to sub-intermediate. All four intermediate shock types share the property that B_{\perp} changes sign; the magnetic field may either increase or decrease in magnitude (see Equation 2.18). It is possible for an intermediate shock to occur at the same velocity as a fast

shock since both are super-intermediate upstream; slow shocks, being sub-intermediate, are unique at a given shock velocity v_s . The nature of intermediate shocks is problematical, and will be discussed further below.

Before considering a general field geometry, we shall look at the special cases of perpendicular and parallel shocks. The angle characterizing the shock is that between \mathbf{B} and the shock normal, $\theta_1 = \tan^{-1}(B_{\perp 1}/B_{\parallel 1})$.

2.2.1 PERPENDICULAR SHOCKS ($\theta_1 = \pi/2$) For the special case of a fluid with $u = P/(\gamma - 1)$ and $B_{\parallel} = 0$, the solution to Equations (2.6–2.11) is fairly simple (e.g. Roberge & Draine 1990). The compression ratio is

$$\frac{\rho_2}{\rho_1} = \frac{2(\gamma + 1)}{D + [D^2 + 4(\gamma + 1)(2 - \gamma)M_A^{-2}]^{1/2}}, \quad (2.19a)$$

$$D \equiv (\gamma - 1) + (2M^{-2} + \gamma M_A^{-2}), \quad (2.19b)$$

where $M_A \equiv v_s/v_{A1}$ is the “Alfvén Mach number” and $M \equiv v_s/c_{s1}$ is the ordinary Mach number. In this case, the only possible shock is a fast shock, with $v_s > u_{F1} = (v_{A1}^2 + c_{s1}^2)^{1/2}$.

2.2.2 PARALLEL SHOCKS ($\theta_1 = 0$) The other limiting case, where $B_{\perp} = 0$, is more subtle. For this case we have $u_F = \max(c_s, v_A)$, $u_S = \min(c_s, v_A)$. For $c_{s1} < v_s$ the jump conditions (2.6–2.11) always admit a purely “hydrodynamic” solution where $B_{\perp} = 0$ throughout; the magnetic field has no dynamic role and the compression ratio is given by (2.19) with $M_A^{-2} = 0$:

$$\frac{\rho_2}{\rho_1} = \frac{\gamma + 1}{\gamma - 1 + 2M^{-2}}. \quad (2.20)$$

If $v_{A1} < c_{s1}$, then this hydrodynamic shock is always a fast shock. If $c_{s1} < v_{A1}$, then the hydrodynamic solution is either a slow, intermediate, or fast shock, depending on the shock velocity.

There is a second solution for parallel shocks, known as a “switch-on” shock, in which the postshock flow acquires a transverse magnetic field B_{\perp} and transverse velocity v_{\perp} [in the frame where $(v_{\perp})_1 = 0$]. The switch-on shock is a fast shock. When it exists, the hydrodynamic shock is an intermediate shock; thus the condition for the existence of a switch-on shock is that an intermediate shock exists as well. The requirement that the hydrodynamic shock be intermediate is that the postshock velocity be sub-intermediate ($v_{\parallel 2} < u_{I2}$). Together with Equation (2.20), this condition implies that the switch-on solution exists provided

$$c_{s1} < v_{A1} < v_s < v_{\text{crit}} \equiv \left[\frac{(\gamma + 1)v_{A1}^2 - 2c_{s1}^2}{\gamma - 1} \right]^{1/2} \quad (2.21)$$

(Priest 1982). For $\gamma = 5/3$, switch-on shocks are restricted to the range $1 < M_A \leq 2$. For radiative shocks ($\gamma \sim 1$), the allowed range of M_A is much greater. Smith (1992, 1993b) has pointed out that radiative quasi-parallel shocks will be “switch-type” for a wide range of conditions, with the final compression limited by magnetic pressure. The compression ratio in a switch-on shock is simply

$$\frac{\rho_2}{\rho_1} = M_A^2. \quad (2.22)$$

From (2.18) we see that a switch-on shock must have $v_{\parallel 2} = u_{l2}$: The post-shock flow velocity equals the intermediate wave velocity. This degeneracy has led Roikhvarger & Syrovatskii (1979) to suggest that the structure of switch-on shocks is dominated by diffusive effects, and that the width grows as the square root of the time.

2.2.3 GENERAL CASE ($0 < \theta_1 < \pi/2$) Consider now the case where the pre-shock magnetic field is neither parallel nor perpendicular ($B_{\parallel}B_{\perp} \neq 0$). For shocks that are sufficiently strong ($M_A \gg 1$, $M \gg 1$), it is possible to approximate the jump conditions (Hollenbach & McKee 1979). For shocks with $\gamma = 5/3$, the magnetic field becomes unimportant at high M_A : For $M_A > 6$, all the terms in the jump conditions involving the magnetic field can be omitted without affecting the values of the downstream density and temperature by more than 30%. For radiative shocks in which the downstream pressure is predominantly magnetic, similar accuracy can be achieved by omitting the terms with v_{\perp} in Equations (2.10) and (2.13) provided $M_A > 5/\tan \theta_1$. For $\gamma > 1$, the compression ratio and postshock temperature have limiting values which are independent of the field:

$$\lim_{M, M_A \rightarrow \infty} \frac{\rho_2}{\rho_1} = \frac{\gamma + 1}{\gamma - 1} \quad (= 4 \text{ for } \gamma = 5/3), \quad (2.23)$$

$$\begin{aligned} \lim_{M, M_A \rightarrow \infty} T_2^{\text{eq}} &= \frac{2(\gamma - 1)}{(\gamma + 1)^2} \frac{\mu v_s^2}{k} \quad \left(= \frac{3}{16} \frac{\mu v_s^2}{k} \text{ for } \gamma = 5/3 \right), \\ &= 1.38 \times 10^5 v_{s7}^2 \text{ K} \quad (\text{for } \mu = [1.4/2.3]m_H), \end{aligned} \quad (2.24)$$

where μ is the mass per particle, all species are assumed to have the same temperature, and $v_{s7} \equiv v_s/10^7 \text{ cm s}^{-1}$.

Shocks that are not strong exhibit more complex behavior. For $u_s < v_s < u_l$, a slow shock is possible in which the gas is compressed but the magnetic field strength decreases; in the limit where $v_s \rightarrow u_l$ this becomes a “switch-off” shock in which $B_{\perp 2} \rightarrow 0$. For $v_s = u_l$ the jump conditions

admit a finite amplitude, noncompressive, nondissipative Alfvén wave (or “rotational discontinuity,” since in effect the magnetic field just rotates by some angle); being reversible, this is not a bona fide shock.

For $u_{11} < v_s < v_{\text{crit}}(\theta_1)$ the jump conditions admit intermediate shocks, in which B_\perp changes sign across the shock. The nature of intermediate shocks is controversial. Some authors (Kantrowitz & Petschek 1966, Landau et al 1984) have rejected these solutions as “nonevolutionary” or “extraneous,” based on the argument that an arbitrary small perturbation at the shock cannot be decomposed into outgoing small-amplitude waves. Since an intermediate shock has $v_s > u_{11}$, it will overtake intermediate waves upstream; on the other hand, such a shock has $v_{\parallel 2} < u_{12}$, so intermediate waves from downstream will catch up to the shock. Therefore an intermediate shock, perturbed by incoming intermediate waves, can only radiate a single intermediate wave, propagating downstream. With only a single outgoing intermediate wave, an arbitrary perturbation at the shock (with both velocity and magnetic field perturbations perpendicular to the original plane of polarization) cannot be decomposed into outgoing waves. This leads to a contradiction: Intermediate waves change the plane of \mathbf{B} , whereas Equation (2.18) requires this plane to remain invariant across the shock. As a result, it is argued, the perturbed intermediate shock will disintegrate into two or more fronts propagating separately. Recently, however, Kennel et al (1990) have shown that the inclusion of viscous or resistive effects in the fluid equations makes the structure of intermediate shocks inherently time-dependent (in contrast to the structure of fast or slow shocks) thus vitiating the conclusions deduced from the time-independent jump conditions. Furthermore, an additional parameter is needed to specify the state of the fluid behind a time-dependent intermediate shock: the angle of rotation of the field. Subsequently, Wu & Kennel (1992) have found that, for time $t \rightarrow \infty$, the width of an intermediate shock broadens as $t^{1/2}$, while its strength decreases as $t^{-1/2}$. In the limit $t \rightarrow \infty$, these time-dependent intermediate shocks evolve into broad, incompressive “rotational discontinuities.”

At present, direct evidence for the existence of intermediate shocks in numerical experiments or in nature is limited. Steinolfson & Hundhausen (1990) found intermediate shocks in their 2-D simulations of coronal mass ejections, but since the restriction to two dimensions does not allow for rotation of the plane of \mathbf{B} , this test is not conclusive. The *Galileo* spacecraft recently observed a plasma structure near Venus which may have been an intermediate shock (Kivelson et al 1991), but again the evidence is not definitive. In any case, it appears that intermediate shocks can exist over only a modest parameter range and are never very strong.

Our understanding of intermediate shocks is far from complete, but

such shocks could have a direct bearing on the structure of weak radiative shocks in the interstellar medium (ISM). If intermediate shocks exist, then in some cases steady shock solutions are not uniquely specified by the upstream and downstream boundary conditions (Draine & McKee 1993): It is sometimes possible to satisfy the boundary conditions by steady solutions containing two or three separate shocks traveling at constant separation, at least one of which is an intermediate shock. When the shocked gas cools radiatively, then the thermal structure and emission spectrum of the overall shock wave will depend upon the physical separation of the multiple shocks; as this may vary without violating the boundary conditions, this means that there may be an infinite number of physically distinct shock solutions for given upstream and downstream boundary conditions! In this case, the actual shock structure will depend upon the complete history of the flow. If steady intermediate shocks are not physically realizable, then these steady multiple shock solutions are nonphysical; if, however, time-dependent intermediate shocks exist which evolve slowly (i.e. are nearly time-independent), then presumably it will be possible to have corresponding multiple shock structures which evolve slowly.

As has been noted by Kantrowitz & Petschek (1966) and Spitzer (1990), additional possibilities arise upon relaxing the requirement that the *overall* shock structure be time-independent. In particular, the initial fast shock could be followed by a slow shock, in which B_{\perp} is *reduced*. The strength of the slow shock will be determined by the downstream boundary conditions. For example, suppose that the downstream boundary conditions required that the transverse magnetic field vanish: $B_{\perp} = 0$. This can be achieved by a switch-off shock—a slow shock propagating at the intermediate speed. It is also possible to satisfy the downstream boundary conditions by inserting large amplitude (but noncompressive and non-dissipative) intermediate waves into the postshock flow. The structure of such a radiative shock is intrinsically time dependent, since both slow shocks and intermediate waves are swept downstream by the flow behind the leading fast shock (except in the limiting case of a switch-on shock, where $v_{\parallel 2} = u_{12}$, so that an intermediate wave can remain a fixed distance behind the leading fast shock). Shortly after the radiative shock forms, the transition to the high compression, low B_{\perp} solution will occur before cooling sets in. Eventually, however, the transition will be swept downstream far enough that it occurs behind the cooling layer, so the cooling will take place at the low density characterizing the gas behind a switch-on shock. When this is the case, the structure of the radiative shock will be equivalent to that of a shock of the same velocity moving into a medium with a significant value of θ_1 .

2.3 Collisionless Shocks

The dissipation of the relative energy of the shocked and unshocked gas occurs in the shock front. For shocks in the atmosphere, this dissipation is due to collisions: The molecules in the shocked and unshocked gases collide, irreversibly converting the energy in relative motion into heat. In interplanetary and interstellar plasmas of proton density $n_i \text{ cm}^{-3}$, however, the distance a proton moving at a velocity $10^7 v_7 \text{ cm s}^{-1}$ must travel before collisions deflect it by 90° is $7.0 \times 10^{14} v_7^4 / n_i \text{ cm}$ (Spitzer 1962). In the solar wind, this distance exceeds the distance from the Earth to the Sun; for young supernova remnants in the ISM, which can expand at velocities exceeding 3000 km s^{-1} ($v_7 = 30$) this distance can exceed the thickness of the cold gas disk of the Galaxy. Observations show that shocks form on much smaller length scales in both cases; the dissipation is effected by the interaction of the particles with “turbulent” electromagnetic fields arising from collective motions of the charged particles, and the shocks are said to be collisionless.

2.3.1 SHOCK STRUCTURE Reviews of collisionless shocks in the solar system can be found in the books edited by Stone & Tsurutani (1985) and Tsurutani & Stone (1985), and we shall draw on their results here. The nature of the shock front in a collisionless shock is determined by the angle θ_1 between the shock normal and the preshock magnetic field. If $\theta_1 \gtrsim 45-50^\circ$, the shock is said to be quasi-perpendicular; otherwise, it is quasi-parallel. In a quasi-perpendicular shock, the magnetic field acts to insulate the upstream region from the downstream region; the motion of the charged particles is primarily gyration around the field rather than streaming along it. If M_A exceeds a critical value which is between 1 and 3, depending on conditions, then the dissipation is associated with ions that are reflected by the compressed magnetic field in the shock before being transmitted downstream. The magnetic field undergoes a large jump in a thin “ramp.” Ahead of the ramp is the “foot,” which is associated with the reflected ions and in which the field begins to rise from its initial value; behind the ramp is the “overshoot” region, in which the magnetic field is larger than its final value by a factor which increases with M_A . The foot and the overshoot region each have a thickness of order the ion Larmor radius. The strongest interplanetary shock observed to date is the bow shock around Uranus, with $M_A = 23$ (Bagenal et al 1987); interstellar shocks can be far stronger, with M_A exceeding 10^2 .

Quasi-parallel shocks are much thicker than quasi-perpendicular shocks and are generally unsteady. Quasi-parallel shocks have an extended “fore-shock” containing electromagnetic waves together with energetic ions which have leaked upstream; a localized jump in density with a thickness

comparable to the ion gyroradius; and a downstream region with large amplitude magnetic turbulence, in which the ions become isotropic. Parker (1961) proposed that shocks of this type would have a structure determined by the magnetic analog of the “firehose” instability: The shocked and unshocked ions constitute two counterstreaming beams with a large stress along the field; just as the rapid flow of water in a hose causes it to flap about, so this flow of ions along the field causes it to become unstable when the difference between the parallel and perpendicular pressures exceeds $B^2/8\pi$. Quest (1988) has generalized this model to include the instability that occurs when the waves can resonate with the gyration of the particles in the foreshock. Because the energetic particles that leak upstream determine the amplitude of the waves that eventually scatter the ions in the localized jump, quasi-parallel shocks are natural sites of particle acceleration (Section 4.2). Quest has shown that this model of quasi-parallel shocks is consistent with numerical simulation, and he has argued that it is consistent with the available observations. However, evidence for reflected ions in quasi-parallel bow shocks, similar to the ions seen in quasi-perpendicular shocks, has been reported by Gosling et al (1989), which suggests that actual quasi-parallel shocks may be somewhat more complicated than the exactly parallel shocks considered by Quest.

The structure of the shock is intimately connected with the issue of how the shock forms in the first place. Astrophysical shocks driven by blast waves or jets often begin with a dense plasma (the piston) exploding into the ambient medium at high velocity. The coupling between the piston and the ambient medium can arise because of charge separation between the electrons and the ions, because of the Larmor motion of the ions, or because of turbulent electromagnetic fields (Cargill 1991). For the quasi-perpendicular case, Larmor coupling ensures that the shock will be set up within a few times Ω_i^{-1} , where Ω_i is the ion gyrofrequency. In the quasi-parallel case, the coupling is expected to be due to the firehose instability, as described above. Although this instability has a characteristic nonlinear growth time $\sim 10\Omega_i^{-1}$, the 1-D simulations reported by Cargill showed that in the exactly parallel case, the shock did not cleanly separate from the piston even after a time of order $100\Omega_i^{-1}$. For the case of the free expansion of a hot piston, a shock was not observed to form at all; whether this would remain true in a more realistic, multi-dimensional simulation including other instabilities [such as electromagnetic streaming instabilities (Weibel 1959)] remains to be seen. In any case, astrophysical time scales are so many orders of magnitude greater than $\Omega_i^{-1} \sim 10^2$ s that it seems likely that quasi-parallel shocks should form and separate from the piston in a time short compared to the overall flow time. A different conclusion

was reached by Spicer et al (1990), who also calculated the X-ray emission that could occur in the time prior to shock formation.

2.3.2 ELECTRON/ION TEMPERATURE RATIO One of the central unsolved problems in the theory of collisionless shocks is the determination of the relative temperatures of the electrons and the ions. The shock jump conditions determine the mean temperature behind the shock front, T_2^{eq} (see Equation 2.24), but not the temperatures of the individual species. (In principle, T_2^{eq} includes the energy in energetic particles, which is unknown and could be substantial—see Section 4.2—but we ignore this complication here.) Since the electrons are generally responsible for the cooling of the plasma, the value of the electron temperature T_{e2} is critical both for understanding the dynamics of the shock and its emitted spectrum. If $T_e = T_i$, the plasma is said to be in equipartition. To measure deviations from equipartition, we shall use the ratio of the electron temperature to the mean temperature T_2^{eq} , which is related to the electron/ion temperature ratio by

$$\frac{T_{e2}}{T_2^{\text{eq}}} = \frac{2.09(T_{e2}/T_{i2})}{1 + 1.09(T_{e2}/T_{i2})} \quad (2.25)$$

for a fully ionized cosmic plasma. Most of the energy in the preshock flow is contained in the ions; the kinetic energy in the streaming of the electrons is less than 1/2000 of the total. The minimum energy transferred from the ions to the electrons is that due to adiabatic compression of the electrons in the shock, and Scudder et al (1986) have argued that this accounts for the heating of the electrons in the Earth's bow shock. Greater heating is possible if the electrons interact with rapidly varying fields. In principle, collisionless heating could result in equipartition, with $T_{e2} = T_2^{\text{eq}}$ (McKee 1974). In a numerical simulation of a very strong shock ($M_A = 50$) in which the electrons were treated as a resistive fluid, Cargill & Papadopoulos (1988) found substantial collisionless heating of the electrons, although not to equipartition; they found $T_{e2}/T_2^{\text{eq}} \simeq 0.36$.

Several observational paths are available for determining the amount of collisionless heating of the electrons in shocks. Observations of the Earth's bow shock are generally consistent with the heating expected from adiabatic compression, and do not indicate any significant collisionless dissipation of energy into the electrons (Stone & Tsurutani 1985). However, the bow shocks at the outer planets are stronger ($M_A \sim 20$) and have lower upstream electron temperatures, and they do indicate significant collisionless heating of the electrons, with $T_e/T_2^{\text{eq}} \sim 0.2$ (Bagenal et al 1987, Moses et al 1985). In a survey of 82 shocks, primarily terrestrial bow shocks but including interplanetary shocks and the Jovian and Uranian

bow shocks, Schwartz et al (1988) found a good correlation between the electron heating ΔT_e and the ion heating ΔT_i , with $\Delta T_e \sim 0.25\Delta T_i$. For the highest values of M_A , the heating was found to be somewhat less, consistent with the result $\Delta T_e \sim 0.1\Delta T_i \sim 0.2T_2^{\text{eq}}$ for the bow shocks of the outer planets. None of these solar system shocks was supersonic relative to the electrons (that is, v_s greater than the electron thermal velocity), although such shocks are expected in supernova remnants.

The most direct observations of the electron temperature in strong interstellar shocks come from X-ray observations of young supernova remnants. (Observations of charge exchange shocks in supernova remnants also provide information on T_{e2} —see Section 4.1.) Inferring the postshock value of T_e is made difficult by the complex structure of many of these remnants, which often have plasmas at several different temperatures. The remnant of SN 1572 (Tycho) appears to have one component of X-ray emission at a temperature of 7×10^7 to 8×10^7 K, which is generally attributed to the shocked ISM (Pravdo & Smith 1979, Smith et al 1988, Hughes 1991); a lower temperature component associated with the shocked ejecta from the supernova is also indicated (Hughes 1991). The velocity of the shock has been variously estimated as 2200 to 3500 km s⁻¹ from observations of the optical lines (Smith et al 1991) to 5200 km s⁻¹ from modeling the X-ray spectrum (Hamilton et al 1986). Even if we adopt the highest estimate for the shock velocity, the lower bound on T_e/T_2^{eq} in Tycho is 0.2. A substantial portion of this electron heating must be collisionless: Coulomb heating of the electrons behind the shock proceeds at a rate

$$\frac{dT_e}{dt} = \frac{T_i - T_e}{t_{\text{eq}}}, \quad (2.26)$$

where the equipartition time is $t_{\text{eq}} = 7.7(T_e^{3/2}/n_H)$ s for a fully ionized cosmic plasma with a Coulomb logarithm of 30 (Spitzer 1962). If all the postshock energy is in the ions ($T_e \ll T_i$, and negligible energy in superthermal particles), then the electron temperature due to collisional heating increases with time as $T_e(\text{coll}) = 1.70 \times 10^7(n_0 t_3 v_{s8}^2)^{2/5}$ K, where t_3 is the age of the remnant in units of 10^3 yr and n_0 refers to the preshock density of H nucleons (cm⁻³). For Tycho, the data (Smith et al 1988, Hamilton et al 1986) imply that $T_e(\text{coll}) \lesssim 3 \times 10^7$ K; since this is significantly less than the observed temperature, collisionless heating is clearly implicated. There is also some evidence for electrons that are substantially hotter than 7×10^7 K—Pravdo & Smith (1979) reported evidence for a component with $T_e \gtrsim 2 \times 10^8$ K. The interpretation of such a hot component is complicated by the fact that collisionlessly heated electrons need not have a Maxwellian distribution (cf Asvarov et al 1990).

2.4 Radiative Shocks

When a shock wave has propagated long enough that radiative losses have cooled the first-shocked material to a small fraction of its initial postshock temperature, then the shock wave is referred to as a “radiative shock.” For a cooling function $\Lambda \propto \rho^2 f(T)$, it is easy to show that, for a given (steady) shock speed, preshock composition, and preshock Alfvén velocity (i.e. fixed $M_A = v_s/v_{A1}$), the postshock temperature will be a function $T(N_H)$ of the cumulative column density $N_H = \int_0^x n_H dx$, where x is the distance from the shock front. Therefore a shock has to propagate a certain column density N_{rad} before it becomes a radiative shock. For strong shocks ($M, M_A \gg 1$), increased preshock magnetic field (i.e. decreased M_A) leads to increased N_{rad} , since the magnetic pressure limits the density increase in the postshock zone, thereby increasing the radiative cooling time $\propto nkT/\Lambda$. Dynamically, a strong shock with a postshock temperature much greater than 10^4 K may be considered to be radiative if the temperature drops to 10^4 K, where the cooling function Λ becomes relatively small. For shocks between 60 and 150 km s⁻¹ with $M_A \gg 1$, this occurs in a column $N_{\text{rad}} \simeq 10^{17.5} v_{s7}^4$ cm⁻² (McKee et al 1987). The hydrogen recombination zone extends well beyond N_{rad} , however, because the plasma recombines at a temperature $T \sim 10^{3.5}\text{--}10^{3.7}$ K. Raymond et al (1988) estimate most of the recombination occurs by $N \simeq 10^{18.5} v_{s7}^2$ cm⁻² for shocks with $80 \lesssim v_s \lesssim 140$ km s⁻¹ and $M_A \approx 10$.

2.4.1 RADIATIVE PRECURSORS When the shocked gas generates ionizing radiation, there will be a region ahead of the shock—the “radiative precursor”—where the gas temperature and composition will be altered. Since the emission from the shocked gas depends upon the composition (and to some extent the temperature) of the material just ahead of the shock transition, iterative techniques are often required to find a self-consistent solution for a steady shock with a radiative precursor. The problem is most delicate when the unperturbed preshock medium is largely neutral, but the radiative precursor is able to appreciably ionize the pre-shock hydrogen and helium. Shull & McKee (1979) showed that the preshock ionization is determined by the ratio of the flux of ionizing photons directed upstream to the flux of particles crossing the shock, $n_0 v_s$. Under the assumption of equipartition between the electrons and ions behind the shock, they showed that steady shocks with $v_s > 110$ km s⁻¹ will fully preionize H and He (to He⁺). The opposite extreme was considered by Ohtani (1980), who found that in the absence of collisionless heating the energy loss to Lyman α excitation keeps T_e so low that a $v_s = 100$ km s⁻¹ shock produces $\sim 10\%$ preionization of H, vs $\sim 70\%$ in the models of Shull & McKee.

Radiative precursors in molecular gas have been studied by Hollenbach & McKee (1989). Once the ionization rises above about 1%, each photoionization of H₂ by photons with energy above 15.4 eV produces two neutral hydrogen atoms by dissociative recombination; these atoms can then be photoionized themselves. Altogether, three ionizing photons are needed to produce two protons. Analytic expressions for the composition of the preshock gas were obtained for shock velocities below the critical value for full preionization.

2.4.2 ISOTHERMAL JUMP CONDITIONS When radiative cooling has been able to remove the bulk of the thermal energy from the postshock fluid, it is often useful to pretend that the postshock fluid cools to a temperature equal to the preshock temperature T_1 . From the standpoint of the fluid dynamics, it is immaterial whether the “lost” energy is in the form of radiated photons or internal degrees of freedom, so that the cold postshock fluid at this point will have the same density, pressure, and flow velocity as would be computed for a fluid with adiabatic index $\gamma = 1$. Then Equation (2.19) gives the isothermal jump conditions for perpendicular shocks:

$$\begin{aligned} \frac{\rho_2}{\rho_1} &= \frac{4}{2M^{-2} + M_A^{-2} + [(2M^{-2} + M_A^{-2})^2 + 8M_A^{-2}]^{1/2}}, \\ &\rightarrow 2^{1/2} M_A \text{ for } 1 \ll M_A \ll M^2, \\ &\rightarrow M^2 \text{ for } 1 \leq M^2 \ll M_A. \end{aligned} \quad (2.27)$$

2.4.3 ATOMIC AND MOLECULAR PROCESSES The structure of an interstellar shock wave depends on the atomic processes affecting the composition of the gas and the energy content. The ionization may be affected by collisional ionization, photoionization, charge exchange, and radiative or dissociative recombination. The molecular content may be affected by collisional dissociation and other chemical reactions. Energy loss from the gas [the $\nabla \cdot \mathbf{F}$ term in Equation (2.3)] results from collisional excitation of atoms, ions, or molecules, followed by radiative decay. Realistic models of interstellar shocks, particularly calculations of emission spectra, or absorption line strengths, therefore depend on accurate knowledge of the network of physical processes.

For collisionless shocks, the major uncertainties have nothing to do with atomic processes, but rather the unknown electron temperature behind the shock (Section 2.3), the unknown fraction of the shock energy going into particle acceleration (Section 4), and the uncertain degree to which grains have been vaporized (Section 6). Until recently, the major uncertainty in atomic processes has been the dielectronic recombination rates, but this

problem has been ameliorated by the work of Romanik (1988, 1993). There are considerably greater uncertainties in the rates needed for shocks in molecular gas. Recent work by Dove & Mandy (1986) and by Dove et al (1987) has improved our knowledge of the collisional dissociation of H₂. Collisional excitation of H₂ by H has been addressed by Mandy & Martin (1992), but further work is needed on this important problem. Continued work is needed on determining cross sections for inelastic collisions of H and H₂ with important coolants and diagnostics, particularly OH (e.g. Dewangan et al 1987), CO (e.g. Flower & Launay 1985, Schinke et al 1985, Viscuso & Chernoff 1988), and H₂O (e.g. Palma et al 1988). Dissociative recombination of H₃⁺ could under some conditions be important, but the rate remains controversial (cf Canosa et al 1991).

2.4.4 SPECTRAL DIAGNOSTICS The detailed emission spectrum of a radiative shock depends upon the shock speed and the physical conditions in the preshock material, and observable emission lines therefore offer valuable shock diagnostics. Shocks in HI regions with $v_s \lesssim 20 \text{ km s}^{-1}$ cool mainly via infrared lines of CII and OI; rotational lines of H₂ are also important if H₂/H $\gtrsim 10^{-3}$ (Field et al 1968). Since $F_{\parallel} \propto n_0 v_s^3$, large values of n_0 are required for the infrared line fluxes to be detectable. At high densities, however, the fractional ionization in neutral regions is generally low, and multi-fluid effects (see Section 3) become important. When $v_s \gtrsim 50 \text{ km s}^{-1}$ the line emission from radiative shocks is detectable even for $n_0 \approx 1$. A number of workers have calculated the expected line emission from $v_s \gtrsim 50 \text{ km s}^{-1}$ radiative shocks (e.g. Cox 1972, Shull & McKee 1979, Binnette et al 1985, Cox & Raymond 1985, Hartigan et al 1987, Raymond et al 1988, Hollenbach & McKee 1989, Neufeld & Dalgarno 1989b). Shock speeds in the range 50–300 km s⁻¹ can be diagnosed using relative strengths of lines such as H α , [OI]6300, [OII]3727, [OIII]5007, OIII]1662, and OIV]1400. There are several respects in which the spectra of $v_s \gtrsim 100 \text{ km s}^{-1}$ radiative shocks differ from those of photoionized gas in HII regions or planetary nebulae (e.g. McKee & Hollenbach 1980, Fesen et al 1985, Graham et al 1987): 1. enhanced [SII] $\lambda\lambda 6717, 6731/\text{H}\alpha$ and [OI] $\lambda\lambda 6300, 6364/\text{H}\alpha$ (because most of the sulfur in photoionized regions is in SIII, and most of the oxygen in OII or OIII); 2. emission from a wider range of ionization states (e.g. [OI] $\lambda\lambda 6300, 6364$, [OII]3727, [OIII] $\lambda\lambda 4959, 5007$), 3. larger [OIII] $\lambda 4363/\lambda\lambda 4959, 5007$ (since the [OIII] emission is from regions which are hot enough to collisionally ionize OII \rightarrow OIII, with electron temperature $T \approx 2 \times 10^4 \text{ K}$); 4. larger [OII] $\lambda 3727/\text{H}\alpha$; 5. larger [FeII] $\lambda 1.644 \mu\text{m}/\text{Br}y 2.166 \mu\text{m}$ (since most of the Fe in photoionized regions is FeIII or FeIV, whereas FeII is an important coolant for shock-heated gas as it cools below 10^4 K). The [OI]63 μm line is generally strong in

radiative shocks, and the [OI]63 μm /[CII]158 μm ratio can often discriminate between shocks and photodissociation regions (Hollenbach & McKee 1989). A word of warning, however: Gas heated by X rays can result in some line ratios (e.g. [FeII]/Br γ) similar to shock-heated regions (Graham et al 1990). Furthermore, $v_s \gtrsim 150 \text{ km s}^{-1}$ radiative shocks are unstable (Section 5.1).

2.4.5 “INCOMPLETE” OR “TRUNCATED” SHOCKS A shock that has not propagated long enough to become radiative will have an emission spectrum differing from that of a radiative shock. If the shock has accumulated a column density N_{H} , then to a good approximation the emission may be taken to be the same as the emission from the portion of the radiative shock having the same N_{H} . This is sometimes referred to as an “incomplete” or “truncated” shock. The cooling time to 10⁴ K is $t_{\text{cool}} = N_{\text{rad}}/n_0 v_s \simeq 10^3 v_{s7}^3/n_0 \text{ yr}$ (McKee et al 1987), so shocks younger than t_{cool} will be incomplete. This has been proposed as an explanation for some filaments in the Cygnus Loop with very large [OIII] $\lambda\lambda 4959, 5007/\text{H}\alpha$ (Fesen et al 1982, Dopita & Binette 1983, Shull & Draine 1987, Raymond et al 1988): The [OIII] emission zone is complete, but the hydrogen recombination zone is not.

2.4.6 TIME-DEPENDENT SHOCKS Theoretical treatments of the structure and emission spectrum of radiative shocks generally have assumed that the flow is time-independent in the shock frame. The jump conditions (2.8)–(2.13) can then be used to determine the conditions at any point behind the shock front in terms of the upstream conditions and the total amount of radiation emitted. However, the assumption of a steady state may not always be valid: Analysis of their observations of the Cygnus Loop led Hester et al (1983) to suggest that the decrease in the pressure behind the blast wave shock could significantly affect the shock spectrum.

The modifications in the jump conditions required for shocks with a time-dependent driving pressure have been obtained by McKee et al (1987), assuming the time dependence to be weak. Consider a plane, perpendicular shock which compresses the gas by a factor χ . The shock velocity v_s is a function of time because the pressure driving the shock changes in a time t_P . The basic assumption of their treatment is that the acceleration of the shocked gas is nearly independent of position, which will be true if magnetosonic waves (i.e. fast waves) can cross the shock in a time short compared to t_P . Now the shock thickness is $v_s \Delta t / \chi$, where Δt is the time since the gas was shocked. Since the magnetosonic velocity is about $v_s / \chi^{1/2}$, their assumption will be satisfied provided $t_P \gtrsim \Delta t / \chi^{1/2}$. For radiative shocks, the compression generally satisfies $\chi \lesssim 10^2$, so this con-

dition is met if $t_p \gtrsim 0.1\Delta t$, which is not very restrictive. Under these conditions, the momentum jump condition (2.11) becomes

$$\left[\rho v_{\parallel}^2 + P + \frac{1}{8\pi} B_{\perp}^2 \right] - v_s \int_0^x \rho(x') dx' = 0, \quad (2.28)$$

where the difference is to be evaluated from just in front of the shock ($x = 0$) to the point x behind it. The mass jump condition (2.8) and the energy equation (2.5) are unaffected by weakly time-dependent shocks. In the usual case in which the shock is decelerating ($v_s < 0$), the pressure drops behind the shock front in order to ensure that the shocked gas decelerates at the same rate; the effect of this pressure gradient is represented by the additional term in the momentum jump condition. In steady radiative shocks, the density increases monotonically behind the shock, but in a decelerating shock the density can decrease as its pressure drops. Such a decrease in density can increase the cooling time of the gas, making the radiating layer of the shock thicker and increasing the likelihood that the shock will be observed to be truncated. The density variation can also affect the intensities of the forbidden lines, but calculations of the spectra of decelerating shocks have yet to be carried out.

2.4.7 THERMAL CONDUCTION Radiative cooling produces a temperature gradient behind the shock front, and this makes it possible for thermal conduction to affect the structure and spectrum of radiative interstellar shocks. The condition for conduction to be important is that the characteristic column density for conduction behind the shock, $N_{\text{cond}} = n_2 \kappa_2 T_2 / (\rho_1 v_s^3 / 2)$, where κ is the conductivity, exceed the cooling column density N_{rad} . For normal abundances, emission line cooling by a plasma in ionization equilibrium gives $N_{\text{cond}}/N_{\text{rad}} \sim 0.005$, so conduction is negligible in that case (Borkowski et al 1989). Conduction can have a modest effect on shock structure when nonequilibrium ionization is taken into account, and it can have a major effect if the cooling rate is enhanced by a high metal abundance (Lacey 1988, Borkowski et al 1989).

Lacey (1988) has considered the effects of conduction on shocks under the assumptions that the electrons and ions remain at the same temperature and that there is no transverse component to the magnetic field. Conduction and radiation together can lower the temperature just behind the shock front (Equation 2.24). He allowed for the effects of saturation of the heat flux (i.e. the breakdown of the small mean free path assumption for the electrons). He found that, in addition to the cases cited above, conduction can have a substantial effect on the structure of very fast shocks, $v_s \gtrsim 3 \times 10^4 \text{ km s}^{-1}$. Borkowski et al (1989) showed that the electrons and ions are often not at the same temperature, and constructed

two-temperature models allowing for the suppression of the heat flux by a transverse magnetic field. Borkowski & Shull (1990) have shown that pure oxygen shocks with thermal conduction can account for the spectra of the oxygen-rich fast moving knots in Cas A. However, they point out that infrared cooling by Ne and/or Si could vitiate this agreement.

2.5 Example: Supernova Blast Wave

Supernova explosions are a major source of interstellar shock waves, and serve to illustrate several different shock wave phenomena. Consider a supernova explosion with an energy $E_0 = 10^{51} E_{51}$ ergs; the ejecta have a range of velocities, with an rms velocity of $\sim 10^4 (E_{51}/M_0)^{1/2}$ km s⁻¹, where M_0 is the ejecta mass in solar units. By a few days after the explosion the ejecta are “cold”, having been cooled by adiabatic expansion; there is some residual heating, including radioactive decay, but the sound speed in the ejecta is $\lesssim 10$ km s⁻¹. As the outer edges of the ejecta run into ambient material, two shocks are formed: a shock wave propagating into the ambient interstellar material, and a “reverse” shock propagating back into, and heating, the ejecta. The outer shock wave gradually decelerates as the reverse shock encounters (and decelerates) more and more of the ejecta. By the time t_M when the blast wave has shocked a mass of ambient gas equal to the mass of the ejecta, the bulk of the ejecta will have been decelerated by the reverse shock and $\sim 2/3$ of the initial kinetic energy will have been thermalized.

Following the free expansion phase, the supernova remnant develops a structure which may be approximated by the Sedov-Taylor similarity solution (Landau & Lifschitz 1959, Ostriker & McKee 1988), and the SNR evolution follows this similarity solution so long as radiative losses have not removed more than a small fraction of the initial energy E_0 . During this “Sedov-Taylor phase” the shock wave is said to be “nonradiative” (even though sufficient radiation may be emitted to provide astronomers with valuable diagnostics); the expansion velocity $v_s \propto (E_{51}/n_0)^{1/5} t^{-3/5}$, and the mean temperature $T \propto (E_{51}/n_0)^{2/5} t^{-6/5}$, where t is the age of the blast wave. Because the collision time for a fully-ionized plasma $t_{\text{coll}} \propto T^{3/2}/n$, we see that $t/t_{\text{coll}} \propto (n_0^2 E_{51})^{1/3} v_s^{-14/3}$, so that there is a critical velocity below which collisions have enough time to be important behind the shock front. In particular, for $v_s \lesssim 180(n_0^2 E_{51})^{1/14}$ km s⁻¹, radiative losses due to collisions are sufficient to cool some of the gas in the remnant to the point that a dense shell forms (Cioffi et al 1988). Subsequently, the shock is said to be “radiative.” As we have seen, whether a shock is radiative or not depends on the ratio of the age of the shock to the radiative cooling time for gas just behind the shock. In Figure 2 we show, in the $v_s - n_H$ plane, the regions in which supernova blast waves tend to be either nonradiative

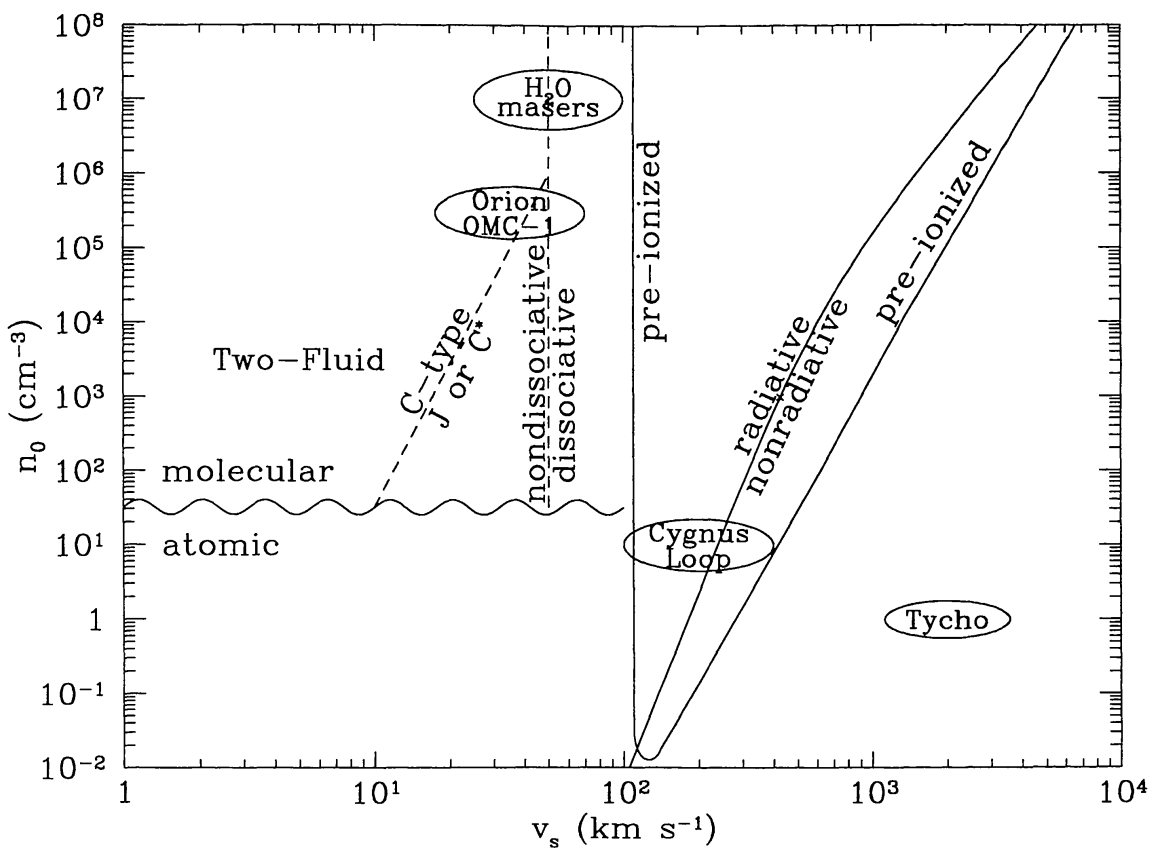


Figure 2 Location of different shock types on the $v_s - n_0$ plane. The line labeled *radiative/nonradiative* separates radiative and nonradiative shocks (for shocks assumed to be driven by a 10^{51} erg supernova explosion). The line labeled *pre-ionized* encloses the conditions under which the radiation emitted by the shock wave is able to pre-ionize initially neutral interstellar gas. Strong two-fluid shocks are possible only if the gas is primarily molecular, which typically requires densities $> 30 \text{ cm}^{-3}$; in atomic gas, strong shocks are J-type. The approximate locations of the Cygnus Loop and Tycho supernova remnants, the H₂ line-emitting region in OMC-1, and the H₂O masers in star-forming regions (Elitzur 1992) are shown.

or radiative. Also shown is the region where the SNR shock is able to fully pre-ionize the preshock medium.

3. MULTIFLUID SHOCKS IN WEAKLY-IONIZED GAS

3.1 *Fluid Equations*

In interstellar clouds the fractional ionization is often small. Even though the charged component of the plasma in these clouds contributes only a small fraction of the mass and pressure, it is dynamically important because

only the charged particles couple to the magnetic field, and the magnetic field is often strong enough to affect the dynamics. When the fractional ionization is low, however, the neutral-ion collision rate is small (charged grains are considered in Section 3.4), and the coupling between ions and neutrals becomes weak enough that it is important to think of the charged and neutral components of the plasma as distinct but interpenetrating fluids. We may safely assume that $\Omega_i \gg n_n \langle \sigma v \rangle$, where $\Omega_i = eB/m_i c$ is the ion cyclotron frequency, n_n is the density of neutral particles, and $\langle \sigma v \rangle$ is the ion-neutral elastic scattering rate coefficient; under these conditions the magnetic field is effectively “frozen” into the charged fluid. The conservation laws for mass, momentum, and energy may be applied separately to each of the fluids, allowing explicitly for exchange of mass, momentum, and energy between the fluids (Mullan 1971, Draine 1980). The fluid equations may be written (Draine 1986a)

$$\frac{\partial}{\partial t} \rho^{(\alpha)} + \frac{\partial}{\partial x_k} [\rho^{(\alpha)} v_k^{(\alpha)}] = S^{(\alpha)} \quad (3.1)$$

$$\frac{\partial}{\partial t} [\rho^{(n)} v_j^{(n)}] + \frac{\partial}{\partial x_k} [\rho^{(n)} v_j^{(n)} v_k^{(n)} + P^{(n)} \delta_{jk} - \sigma_{jk}^{(n)}] = F_j^{(ni)}, \quad (3.2)$$

$$\begin{aligned} \frac{\partial}{\partial t} [\rho^{(i)} v_j^{(i)}] + \frac{\partial}{\partial x_k} \left[\rho^{(i)} v_j^{(i)} v_k^{(i)} + (P^{(i)} + P^{(e)}) \delta_{jk} \right. \\ \left. - \sigma_{jk}^{(i)} + \frac{B^2}{8\pi} \delta_{jk} - \frac{1}{4\pi} B_j B_k \right] = -F_j^{(ni)} \end{aligned} \quad (3.3)$$

$$\frac{\partial}{\partial t} u^{(\alpha)} + \frac{\partial}{\partial x_j} [u^{(\alpha)} v_j^{(\alpha)}] + [P^{(\alpha)} \delta_{jk} - \sigma_{jk}^{(\alpha)}] \frac{\partial v_j^{(\alpha)}}{\partial x_k} + \Lambda^{(\alpha)} = \sum_{\beta \neq \alpha} G^{(\alpha\beta)} \quad (3.4)$$

where α labels the components, both neutral and charged. The collisional coupling between the fluids is described by: $S^{(n)} = -S^{(i)}$, the net rate per volume at which ion mass is converted into neutral mass (including the effects of recombination, collisional ionization, photoionization, and charge exchange); $F^{(ni)}$, the rate per volume of momentum transfer from the ions to the neutrals (including the effects of recombination, elastic scattering, etc); and $G^{(\alpha\beta)}$, the net rate per volume at which the energy density $u^{(\alpha)}$ is changed due to the effects of fluid β (including the thermal energy created by ion-neutral elastic scattering, etc). When plane-parallel, steady flow is assumed these equations may be simplified (Draine 1986a).

3.2 Shock Structure

The Alfvén velocity in interstellar molecular clouds is about $v_A \simeq 2 \text{ km s}^{-1}$, with a scatter of about a factor 3 (Heiles et al 1992); the corresponding

field is $B \sim 1.1 (n_{\text{H}}/\text{cm}^{-3})^{1/2} \mu\text{G}$. The Alfvén velocity in the ionized component of the plasma is then $v_{\text{A}}^{(\text{i})} = B/(4\pi\rho^{(\text{i})})^{1/2} \approx 100 (x_{\text{e}}/10^{-4})^{-1/2} \text{ km s}^{-1}$. For $\theta \neq 0$ the plasma supports compressive “fast” waves with propagation speed $u_{\text{F}}^{(\text{i})} \approx v_{\text{A}}^{(\text{i})}$. Ion-neutral collisions act to damp these waves, but because of this large effective signal speed, the ions are able to communicate ahead of shocks with $v_s < u_{\text{F}}^{(\text{i})} \approx v_{\text{A}}^{(\text{i})}$; from the standpoint of the ions there is no hydrodynamic surprise, and the shock cannot contain a discontinuity in the ion fluid. Such shocks are said to have a “magnetic precursor” (Draine 1980).

Because the ions and neutrals are differentially accelerated, they may have large relative streaming velocities in the shock, a phenomenon referred to as ion-neutral “slip,” or “ambipolar diffusion.” Ion-neutral collisions then heat and accelerate (or decelerate) both ion and neutral fluids. The resulting shock structure will take one of three generic forms (Figure 3). If the neutral fluid remains cold (either because the shock itself is very weak, or because radiative cooling is able to remove the heat dissipated by ion-neutral collisions), then the neutral fluid itself may remain

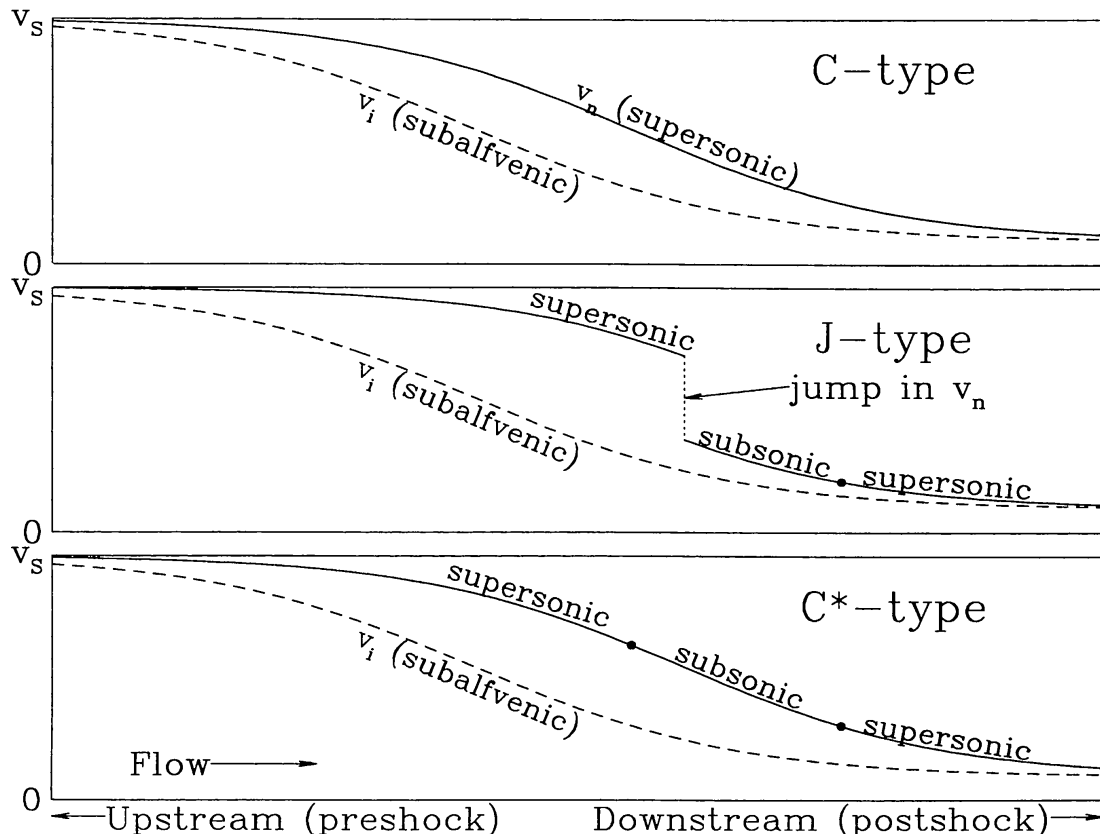


Figure 3 Schematic structure of two-fluid shock waves showing velocities of the neutral and ionized fluids relative to the shock front. Three types of solutions are possible: C-type, J-type, and C*-type.

everywhere supersonic; in this case neither the neutral fluid nor the ion fluid have “critical points” where the flow is transonic; such shocks are termed “C-type” (Draine 1980) since all of the flow variables are continuous. If, however, the heating by ion-neutral collisions raises the neutral gas temperature—and therefore the neutral sound speed—sufficiently so that the neutral flow (which is supersonic far upstream) becomes subsonic, then two possibilities exist. The neutral flow may make the supersonic → subsonic transition by means of a collisional “subshock” (with a thickness of order the neutral mean free path, and with energy dissipation and entropy generation within the subshock dominated by molecular viscosity)—such a shock is termed “J-type,” since it contains a “jump” in the neutral hydrodynamic variables. Under some circumstances, however, it is possible for the neutral fluid to make the supersonic → subsonic transition smoothly—such shocks are termed “C*-type” (Chernoff 1987, Roberge & Draine 1990). The domains of C-type, J-type, and C*-type shocks have been approximately delineated (Chernoff 1987, Hollenbach et al 1989, Chernoff & McKee 1990, Roberge & Draine 1990).

It should be stressed that both far upstream and far downstream from the shock the ion and neutral fluids are always comoving and close to equipartition, so that (aside from possible changes in chemical composition) these multifluid shocks obey the same *overall* jump conditions (relating fluid conditions far upstream and downstream) as single-fluid MHD shocks. The multifluid nature is important only insofar as the structure of the shock transition itself matters. What makes these multifluid shocks very different is that ion-neutral slip provides a “frictional” mechanism which can convert the directed kinetic energy of the upstream flow into heat at a rate which (because of the scarcity of ions) is low enough that radiative cooling may be able to maintain the fluids at temperatures far below the temperature T_2^{eq} which would have been attained in the absence of cooling. In effect this provides a situation where the “shock transition” and the “radiative cooling zone” (Figure 1) coincide. As a result, (a) molecules can be accelerated to high velocities without being thermally dissociated; and (b) the power radiated by such shocks will largely appear in atomic and ionic fine structure lines, and in rotation-vibration transitions of molecules. Since these are the characteristics of C-type shocks, Hollenbach et al (1989) have termed multifluid shocks in weakly ionized gas “C_{eff}” shocks, even though technically they may be C-type, C*-type, or have a weak jump.

3.3 Atomic and Molecular Processes

The coupling of the ion and neutral fluids plays a crucial role in the shock structure. This coupling is mainly due to three processes: ion-neutral elastic

scattering, charge exchange, and scattering by charged dust grains. For elastic scattering, the force density acting on species α due to interaction with species β is

$$F_j^{\alpha\beta} = \frac{\rho^{(\alpha)}\rho^{(\beta)}}{(m_\alpha+m_\beta)} \langle\sigma v\rangle_{\alpha\beta} (v_j^{(\beta)} - v_j^{(\alpha)}) \quad (3.5)$$

where m_α and m_β are the masses of species α and β , and $\langle\sigma v\rangle_{\alpha\beta}$ is the “momentum-transfer rate coefficient” for α - β scattering. For ion-neutral scattering this rate coefficient is approximately (Draine et al 1983)

$$\langle\sigma v\rangle_{\alpha\beta} \approx 1.9 \times 10^{-9} \text{ cm}^3 \text{ s}^{-1} \quad \text{for } v_{\text{rel}} \equiv |\mathbf{v}^{(n)} - \mathbf{v}^{(i)}| \lesssim 15 \text{ km s}^{-1}. \quad (3.6)$$

Charge exchange of H^+ with H is important when H^+ constitutes a significant fraction of the ions; charge exchange can be regarded as simply another form of elastic scattering with a momentum transfer rate coefficient $\langle\sigma v\rangle = 2\langle\sigma_x v\rangle$, where $\langle\sigma_x v\rangle \approx 8.4 \times 10^{-9} T_4^{0.4} \text{ cm}^3 \text{ s}^{-1}$ is the rate coefficient for charge exchange. Elastic scattering will lead to heat exchange between species α and β if they are at different temperatures. In addition, if the two species are streaming relative to one another, there will be heat generation. The result is a source term of the form

$$G^{(\alpha\beta)} = \frac{\rho^{(\alpha)}\rho^{(\beta)}}{(m_\alpha+m_\beta)^2} \langle\sigma v\rangle_{\alpha\beta} [3A(s)k(T_\beta - T_\alpha) + m_\beta v_{\text{rel}}^2], \quad (3.7)$$

where $s^2 \equiv m_\alpha m_\beta v_{\text{rel}}^2 / 2k(m_\alpha T_\beta + m_\beta T_\alpha)$ and in general $A(s) \approx 1$ for $s^2 \ll 1$. For the particular form $\langle\sigma v\rangle = \text{constant}$, $A(s) = 1$ independent of s (Draine 1986a).

Because of the low mass of the electrons, momentum transfer between neutrals and electrons—and the associated dissipation—is normally negligible. The detailed structure of C_{eff} shock waves depends on the ability of the total cooling function $\Lambda^{(e)} + \Lambda^{(i)} + \Lambda^{(n)}$ to compete with the total heating rate

$$G^{(\text{in})} + G^{(\text{ni})} = \sum_{\alpha \in i} \sum_{\beta \in n} \frac{\rho^{(\alpha)}\rho^{(\beta)}}{m_\alpha+m_\beta} \langle\sigma v\rangle_{\alpha\beta} v_{\text{rel}}^2. \quad (3.8)$$

So long as the temperature remains below ~ 5000 K, radiative cooling in these shocks is dominated by fine-structure excitation of atoms and ions (e.g. [CII]157 μm , [OI]63 μm) and rotational and vibrational lines of H_2 , CO, OH, and H_2O . As seen above, under some circumstances the cooling processes may be able to balance the rate of energy dissipation by ion-neutral slip, resulting in a C_{eff} shock. Under these conditions, the peak temperature attained in the shock is of course determined by the detailed behavior of the cooling functions Λ ; models of C_{eff} shocks are therefore sensitive to uncertainties in the inelastic cross sections. Many very impor-

tant inelastic cross sections (e.g. rotational excitation of H₂ by H) are still quite uncertain, though progress is being made (e.g. Mandy & Martin 1992).

3.4 Role of Dust Grains

Dust grains typically account for $\sim 0.6\%$ of the total mass of the medium. Under a broad range of conditions, grains (at least the larger grains, accounting for most of the mass) are charged, either positively (by photoelectric emission due to UV photons in diffuse clouds) or negatively (by collisions with electrons). Because of this charge, the grains are coupled to the magnetic field on a time scale $\Omega_{\text{gr}}^{-1} = Mc/QB$ (where Q/M is the grain charge-to-mass ratio), but they are also strongly coupled to the neutral gas by ordinary gas drag (i.e. collisions with atoms or molecules) on a time scale τ_{drag} . A further complication is the fact that the grain charge fluctuates on a time scale τ_Q . The resulting grain dynamics is complex, and determined by the relative magnitudes of Ω_{gr}^{-1} , τ_{drag} , τ_Q , and the time scale L/v_s , where L is the length scale over which the fluid velocities and densities vary in the shock.

The grains may have two different important effects: as a nonnegligible carrier of momentum and kinetic energy (Section 6.3), and, since they are coupled to both the magnetized plasma and the neutral gas, as an important source of momentum transfer between these fluids. Grains may be more important than ordinary ion-neutral scattering when the ion fraction $x_e \lesssim 10^{-6}$ (Draine 1980, Draine et al 1983). The magnitude of this effect is sensitive to the grain size distribution. The state of motion of the grains further depends on the grain charge, which in turn depends on rates of photoelectric emission, collisional charging by free ions and electrons, and grain-grain collisions. Most calculations of multifluid shocks have been for typical molecular cloud densities, for which the charge is carried primarily by ions and electrons. The extension to higher densities, where the charge is primarily carried by the grains, has been considered by Chernoff (1985), Havnes et al (1987), and Pilipp et al (1990). Finally, most estimates of the state of motion of the dust (e.g. Draine 1980) have neglected grain inertia (i.e. have assumed the net force on a grain to vanish); however, as we now discuss, grain inertia is not necessarily negligible.

Even though the grains account for less than 1% of the total mass, they have a mass much greater than the mass of the ions (for fractional ionizations $\ll 10^{-2}$). If, therefore, the grains were able to “load” the magnetic field, the resulting Alfvén velocity would be much lower than the Alfvén velocity $B/(4\pi\rho^{(i)})^{1/2}$ estimated using the ion mass density (McKee et al 1984); if the total grain mass were included in estimating the preshock Alfvén velocity, the resulting value would be only $B/(4\pi\rho)^{1/2} \approx 10v_A \sim$

20 km s⁻¹, and the ion fluid could not sustain a “magnetic precursor” in shocks with $v_s \gtrsim 20$ km s⁻¹. Since the grains have only a finite coupling to the magnetic field (i.e. $\Omega_{\text{gr}}L/v_s$ is not necessarily very large compared to 1), explicit calculations will be required to reveal to what degree the grains will interfere with development of a magnetic precursor. When the Mach number of the grain fluid exceeds unity and the drag is not too great ($\Omega_{\text{gr}}\tau_{\text{drag}} > 1$), the grain fluid can undergo a shock (Chernoff 1985, Pilipp et al 1990). A substantial complication is that the grains have a wide range of masses and therefore of Ω_{gr} . Pilipp et al (1990) have shown that lumping all the grains together in a single fluid is valid only over a limited range of parameters.

3.5 Length Scales

In a weakly ionized medium, the inertia of the charged particles is negligible compared to that of the neutrals, and the pressure of the charged particles is negligible compared to that of the magnetic field. For a steady, perpendicular shock ($B_{\parallel} = 0$), the overall jump condition (2.11) gives

$$\Delta B_{\perp}^2 \approx 8\pi\rho_0 v_s^2, \quad (3.9)$$

where we have assumed the overall shock to be strong and radiative so that $v_2 \ll v_s$, with the final compression limited by magnetic pressure. From the ion momentum Equation (3.3) we have (letting $\nabla \approx L^{-1}$)

$$\frac{\Delta B_{\perp}^2}{8\pi L} \approx \frac{\rho^{(\text{n})}\rho^{(\text{i})}}{m_{\text{n}}+m_{\text{i}}} \langle \sigma v \rangle v_{\text{rel}}. \quad (3.10)$$

If the downstream fluid is supported by magnetic pressure, then the compression ratio is $\sim 2^{1/2}M_A$ (cf Equation 2.27) so that the product $\rho^{(\text{n})}\rho^{(\text{i})}$ increases by a factor $2M_A^2$ from preshock to postshock. Using the geometric mean of preshock and postshock values in (3.10), we obtain an estimate for the shock thickness L :

$$L \approx \frac{2^{1/2}(m_{\text{n}}+m_{\text{i}})v_s}{M_A\rho_1^{(\text{i})}\langle \sigma v \rangle} \left(\frac{v_s}{2v_{\text{rel}}} \right), \quad (3.11)$$

where the result depends on the value taken for the slip velocity v_{rel} ; v_{rel} actually depends upon the efficacy of cooling in the shock, but $v_{\text{rel}} \approx v_s/2$ is a reasonable estimate. Thus

$$L \approx 7 \times 10^{15} \left(\frac{v_{\text{A1}}}{\text{km s}^{-1}} \right) \left(\frac{10^{-2} \text{ cm}^{-3}}{n_1^{(\text{i})}} \right) \text{cm}, \quad (3.12)$$

where $n_i^{(i)}$ is the preshock number density of ions, and we have assumed $\langle \sigma v \rangle = 2 \times 10^{-9} \text{ cm}^3 \text{ s}^{-1}$.

3.6 Critical Ionization Velocity

As part of a theory for the origin of the solar system, Alfvén (1954) proposed that a neutral gas streaming across a magnetized plasma faster than the critical velocity defined by

$$\frac{1}{2}m_n v_{\text{crit}}^2 = I, \quad (3.13)$$

where I is the ionization energy of the neutral species, would be rapidly ionized in a process akin to an electrical discharge. Since the rate of collisional ionization by electrons is much greater than that by ions, he supposed that instabilities would transfer energy from the ions to the electrons, which would then produce more ions, etc. Experiments have confirmed the existence of this phenomenon in the laboratory; experiments in space have had mixed results (see the review by Newell 1985; for a recent discussion of the space experiments, see Papadopoulos 1992). The instability responsible for transferring the energy from the ions to the electrons is believed to be the lower hybrid instability (sometimes termed the modified two-stream instability), an electrostatic streaming instability with a wavelength intermediate between the electron gyroradius and the ion gyroradius, so that the electrons are tied to the field but the ions are not. Formisano et al (1982) have argued that the outcome of the instability depends on the ratio of the growth rate of the ionization, $n\sigma_{\text{ion}}v$, to the ion gyrofrequency Ω_i . For rapid ionization ($n\sigma_{\text{ion}}v \gg \Omega_i$), the magnetic field does not affect the ion motion as the discharge develops and quasi-linear theory predicts that 2/3 of the ion energy will be transferred to the electrons. On the other hand, for slow ionization [$n\sigma_{\text{ion}}v \ll (m_e/m_i)^{1/2}\Omega_i$], they find that only 2.5% of the ion energy is transferred to the electrons. In molecular clouds in the ISM, which typically have $v_A \sim 2 \text{ km s}^{-1}$ (Heiles et al 1992), this slow ionization criterion is satisfied for $n \lesssim 10^6 \text{ cm}^{-3}$.

C_{eff} shocks can create the conditions necessary for critical ionization, since the shock drives the ionized component of the plasma through the neutrals at a velocity approaching the shock velocity. If the ionization of the plasma begins to rise rapidly, the shock becomes a strong J-shock: The rapid rise in the ionization causes a corresponding increase in the heating rate ($\propto \rho^{(n)}\rho^{(i)}$), which leads to dissociation of the gas, a corresponding drop in the cooling rate, and runaway heating and ionization (although the gas remains primarily neutral). This breakdown has been studied by Chernoff et al (1982), Draine et al (1983), Hollenbach et al (1989), Chernoff & McKee (1990), and Smith & Brand (1990). Chernoff et al (1982), Hollenbach et al (1989), and Chernoff & McKee (1990) adopted the

collisionless heating rate appropriate for low ionization from Formisano et al (1982), but found that it had little effect. All studies found that breakdown occurred in molecular gas in the ISM at shock velocities of order $40\text{--}50 \text{ km s}^{-1}$. This velocity for breakdown due to collisional ionization is quite close to that predicted by Alfvén: allowing for both dissociation and ionization, and including helium with $n(\text{He}) = 0.1n(\text{H})$, Equation (3.13) gives a critical ionization velocity $v_{\text{crit}} \simeq 50 \text{ km s}^{-1}$.

3.7 Magnetic Precursors to J-Type Shocks

Even when cooling is not sufficiently rapid to form a C_{eff} shock, a shock with $v_s < u_{\text{F1}}^{(i)}$ will have a magnetic precursor region where ions and electrons stream through the neutral fluid. Since an element of the neutral fluid will be subject to a gradual increase in the heating rate, the temperature in the precursor will also rise gradually from the ambient value, and even in a very fast shock there may be associated emission from molecules or atoms present in the ambient medium.

The magnetic precursor length scale $L_{\text{mp}} \equiv |d \ln v^{(i)} / dx|^{-1}$ may be estimated at the point where $v^{(i)} = v_s/2$, assuming a perpendicular shock ($B_{\parallel} = 0$), $v^{(n)} \approx v_s$, and neglecting the inertia and pressure of the ions compared to the magnetic pressure. Then from (3.3) and (3.5) one finds (Draine 1980)

$$L_{\text{mp}} = \frac{(m_n + m_i)B_1^2}{\pi \rho_i^{(i)} \rho_i^{(n)} \langle \sigma v \rangle v_s} \approx 2 \times 10^{14} \left(\frac{v_{\text{A1}}}{\text{km s}^{-1}} \right)^2 \left(\frac{10^{-2} \text{ cm}^{-3}}{n_i^{(i)}} \right) v_s^{-1} \text{ cm.} \quad (3.14)$$

Equation (3.14) assumes that the fractional ionization remains constant. As discussed in Section 3.6, the precursor will be present only so long as v_{rel} does not exceed $\sim 40 \text{ km s}^{-1}$; above the “breakdown velocity” runaway ionization will occur, the heating rate $\propto \rho^{(n)} \rho^{(i)}$ will increase rapidly, and a viscous subshock is likely to develop.

Magnetic precursors to $v_s \approx 100 \text{ km s}^{-1}$ shocks have been proposed to explain the H_2 emission in Herbig-Haro objects (Hartigan et al 1989, Curiel 1992), and Graham et al (1991) have proposed that magnetic precursors to $v_s \approx 170 \text{ km s}^{-1}$ shocks may account for H_2 emission from several filaments in the Cygnus Loop supernova remnant.

Thus far, only very simplified models have been used to estimate the line emission from these proposed precursors. These models seem to offer an attractive explanation for a number of observations, but raise several issues:

1. The large streaming velocities $\sim v_s/2 \gtrsim 50 \text{ km s}^{-1}$ proposed for these precursors seem dangerously large (cf Section 3.6) and it will be of

- interest to see more detailed calculations of the heating, chemistry, and ionization in the precursors. It seems likely that precursors to such fast shocks will be truncated by “breakdown” when v_{rel} reaches $\sim 40 \text{ km s}^{-1}$.
2. The models require that the Alfvén speed for the charged particles $(\rho^{(n)}/\rho^{(i)})^{1/2}v_A$ must exceed v_s at the leading edge of the precursor; for v_s as large as $100\text{--}170 \text{ km s}^{-1}$, this is possible only if the fractional ionization remains extremely low. In diffuse regions (e.g. the Cygnus Loop filaments) with starlight photoionization of carbon [$n(\text{C}^+)/n_{\text{H}} \approx 2 \times 10^{-4}$] the Alfvén speed for the ion-electron fluid will be only $24v_{A1}$. Ionization of only 0.2% of the preshock hydrogen will reduce this further to only $18v_{A1}$. Therefore magnetic precursors to these fast shocks are possible only if the preshock Alfvén speed is considerably greater than the value $\sim 2 \text{ km s}^{-1}$ thought to be typical of neutral regions *and* there is no appreciable ionization of hydrogen by a radiative precursor. For shock speeds $v_s \gtrsim 100 \text{ km s}^{-1}$ these seem difficult conditions to fulfill.
 3. As mentioned in Section 3.4, charged dust grains may ‘load’ the magnetic field and further reduce the effective Alfvén speed for the charged fluid.

More detailed modeling of magnetic precursors to fast J-type shocks will be of considerable value to clarify these issues.

3.8 Numerical Modeling

Steady, plane-parallel C-type shock models are (hydrodynamically) straightforward: They present an initial value problem where one simply integrates a set of coupled ordinary differential equations. If there are heavy computational demands, they will arise from the need to integrate “stiff” equations for chemistry or heat exchange between fluids, or the need to compute level populations for H₂, etc.

J-type or C*-type flows are much more difficult: Here the neutral fluid makes a supersonic → subsonic transition, so the flow has a critical point where various derivatives (e.g. $dv^{(n)}/dx$) are ill-defined. In fact, for common parameters the neutral flow downstream will be supersonic (cf Figure 3) and there will be a subsonic → supersonic transition. In the case of J-type shocks one must insert a viscous subshock (jump) to effect the supersonic → subsonic transition; the location of this subshock must be chosen to permit the downstream boundary conditions to be satisfied. Similarly, in C*-type shocks there are an infinite number of trajectories emerging from the first sonic point; the physically correct trajectory is determined by conditions downstream. Solutions to these “two-point boundary value problems” may be found using “relaxation” techniques (e.g. Draine 1980) or “shooting” methods (Roberge & Draine 1990). Because J-type and C*-

type flows are so much more difficult to compute, there has thus far been relatively little exploration of these solutions.

4. MULTIFLUID SHOCKS IN IONIZED GAS

4.1 *Nonradiative Shocks in Partially Neutral Gas*

In a partially neutral gas, multifluid shocks can occur which are quite different from the C-shocks discussed above. In this case, the shock is supersonic with respect to both the ionized and the neutral media. The ionized gas undergoes a collisionless shock that heats and accelerates the ions and electrons in a very short distance (Section 2.3). The neutrals are unaffected by this collisionless shock, however, since they interact with the shocked plasma only through collisions. The spectrum produced by the neutral gas while being ionized accounts for the observations of a number of supernova remnants (SNRs) and provides a powerful diagnostic for the structure of interstellar shocks (Chevalier & Raymond 1978, Chevalier et al 1980, R. C. Smith et al 1991). Raymond (1991) has reviewed this topic recently, so our discussion will be brief.

In order for the gas ahead of the shock to be partially neutral, it cannot have been fully ionized by the radiative precursor (Section 2.4.1). Nonradiative shocks usually satisfy this condition (see Figure 2). Neutral atoms which find themselves behind the shock front will be subject to collisional excitation, producing narrow emission lines at the velocity of the unshocked gas. They are also subject to charge exchange, which produces a population of fast H atoms that emit broad emission lines centered at about the velocity of the shocked plasma. The profile of the broad lines directly reflects the velocity distribution of the collisionlessly heated ions; by combining the measured line width with observations of the proper motion, one can estimate the distance to the shock (Chevalier et al 1980). The cross section for charge exchange is $\sigma_x \simeq 10^{-15} \text{ cm}^2$ at a velocity of 10^3 km s^{-1} , so the thickness of the charge exchange layer [$\sim 1/(n\sigma_x)$] is quite small by astronomical standards. In most nebulae, emission from the metals competes with that from the hydrogen because either the gas is too cool to collisionally excite the Balmer lines or the hydrogen is fully ionized. That is not the case in a $v_s \gtrsim 100 \text{ km s}^{-1}$ nonradiative shock: The electrons are quite hot, neutral hydrogen is abundant, and the emission from the metals is smaller than that from hydrogen by about two orders of magnitude. For this reason, the optical spectrum is dominated by the Balmer lines of hydrogen, and SNRs displaying such spectra, such as Tycho and SN 1006, are referred to as “Balmer-dominated.” Remnants with radiative shocks, such as the Cygnus Loop, sometimes show Balmer-dominated shocks outside the main radiative shocks (Raymond et al 1983).

Bychkov & Lebedev (1979) discussed Balmer-dominated shocks without distinguishing between the broad and narrow components of the line profile. Such shocks can also be detected in absorption in the Lyman lines of hydrogen (Cowie et al 1979).

The ratio of the broad and narrow components of the lines depends on the shock velocity and on the electron-ion temperature ratio behind the shock. Observations show that the narrow component of H α is generally brighter than the broad component (R. C. Smith et al 1991). Models in which the electrons undergo substantial collisionless heating at the shock front, but do not reach equipartition (as discussed in Section 2.3), may account for the observations (R. C. Smith et al 1991).

4.2 Particle Acceleration

Interstellar plasma is filled with relativistic particles—the cosmic rays—that have an energy density comparable to that of the thermal gas and the magnetic field threading it. Over a decade ago it was shown that the cosmic rays could originate in shocks by first order Fermi acceleration (Axford et al 1977, Bell 1978, Blandford & Ostriker 1978, Krymsky 1977), and more recently it has been realized that these relativistic particles can have a profound effect on the structure of the shock itself. Observations of shocks in the Solar System have confirmed some of the key aspects of the theory (e.g. Ellison et al 1990). For a more detailed account of particle acceleration and its effects on shocks, readers are referred to two excellent recent reviews by Blandford & Eichler (1987) and by Jones & Ellison (1991).

4.2.1 PHYSICS OF SHOCK ACCELERATION When particles are trapped in a medium undergoing compression, they accelerate; if they have a constant probability of escaping, their momentum distribution becomes a power-law (Fermi 1949). Let t_{acc} be the acceleration time, t_{esc} be the escape time, and $f(p)dp$ be the density of particles in the momentum range dp . The distribution of particle momenta in a steady state is then

$$f(p) \propto p^{-(1+t_{\text{acc}}/t_{\text{esc}})} \equiv p^{-\alpha}. \quad (4.1)$$

The generality of this argument suggests that it may account for the particle spectra observed in astrophysical and space plasmas. However, the power-law index appears to depend on the details on the acceleration process and the structure of the source, whereas particle spectra in astrophysics tend to fall in a relatively narrow range around $\alpha \sim 2.5$ (Blandford & Eichler 1987).

In a shock, the compression is due to the convergence of the flows of the shocked and unshocked plasmas at a relative velocity $\Delta v \equiv v_1 - v_2$. To determine the resulting particle spectrum, we follow the test particle

approach developed by Bell (1978). We assume that the ambient magnetic field is parallel to the shock velocity, and that fluctuations in the field, either preexisting or self-generated, are sufficient to cause the distribution of superthermal particles to be essentially isotropic in the fluid frame. Each time a particle with velocity $w \gg v_1$ is reflected from the shock, its momentum is increased by $(4p\Delta v/3w)$, where the factor 4/3 allows for an average over angles. If t_{refl} is the mean time between reflections, then the acceleration time is

$$t_{\text{acc}} \equiv \left(\frac{d \ln p}{dt} \right)^{-1} = t_{\text{refl}} \left(\frac{4\Delta v}{3w} \right)^{-1}. \quad (4.2)$$

The postshock gas is assumed to be uniform, so $f(p) = f_2(p)$ is constant behind the shock; since the accelerated particles see the shock front as a discontinuity, the distribution function at the shock front is $f_2(p)$ as well. Because the accelerating particles are assumed to be isotropic, their flux from the upstream side to the downstream side of the shock is $(w/4)f_2(p)dp$; on the other hand, the mean flux behind the shock is much smaller, $v_2f_2(p)dp$. Let $r \equiv v_1/v_2$ be the shock compression. We infer that only a fraction $4v_2/w = 4v_1/rw$ of the particles can escape downstream at each reflection; most of the particles must return back upstream to undergo another step in the acceleration process. The escape time t_{esc} is simply the reflection time divided by this fraction, so that $t_{\text{acc}}/t_{\text{esc}} = 3/(r-1)$. We conclude that the momentum distribution of the accelerated particles is

$$f(p) \propto p^{-(r+2)/(r-1)}. \quad (4.3)$$

This argument is quite general, and applies to both nonrelativistic and relativistic particles; more rigorous derivations can be found in the reviews cited above. The accelerated particles are expected to be isotropic in the wave frame, which may differ from the fluid frame if the waves have a net direction of propagation; in this case the velocities v_1 and v_2 entering the definition of the compression ratio r are to be interpreted as the velocities of this frame on the two sides of the shock (Bell 1978).

Several key assumptions went into the derivation of Equation (4.3). First, the shock must appear as a discontinuity—its thickness must be small compared to the mean free path (λ) for scattering the superthermal particles in the fluctuating magnetic field. For nonrelativistic shocks this condition is readily satisfied if there is a preexisting population of superthermal particles, but the process by which thermal particles are boosted to superthermal energies—the injection problem—remains unclear. This problem is particularly acute for electrons (which, via synchrotron emission from SNRs, provide the best direct observational evidence for shock

acceleration) since they must be accelerated to relatively high energies before their Larmor radius is greater than that of a thermal proton (e.g. Ellison & Reynolds 1991, see Levinson 1992 for a possible solution to this problem). Second, the mean free path must be small compared to the size of the system so that the shock is effectively planar and the particles cannot escape. Third, the particle velocities must be large compared to the shock velocity, so that they are approximately isotropic in the shock frame. Finally, this derivation assumes that the field is approximately parallel to the shock velocity. Jokipii (1987) has argued that the shock acceleration process can be even more efficient if the field is nearly perpendicular to the shock velocity. Direct observational confirmation for Jokipii's conjecture is lacking at present. In the absence of such scattering, energetic particles crossing a perpendicular shock will be accelerated, on average, just enough to conserve their magnetic moment (Pesses 1981).

The contribution to the pressure from particles in the logarithmic momentum range $d \ln p$ is

$$\frac{dP_{\text{cr}}}{d \ln p} = \left(\frac{pw}{3} \right) p f(p) \propto w p^{(r-4)/(r-1)}. \quad (4.4)$$

A strong shock in a $\gamma = 5/3$ gas has $r = 4$ and $\alpha = 2$; for such a shock, the partial pressure of relativistic cosmic rays is constant. For nonrelativistic cosmic rays, the partial pressure increases with momentum so long as $r > 5/2$.

The scattering of the accelerated particles can be modeled as a diffusion process with diffusion coefficient κ . The cosmic rays will diffuse upstream a distance L ahead of the shock until the diffusion current $\kappa \partial f / \partial x \equiv \kappa f / L$ equals the rate at which the particles are being swept downstream by the unshocked gas, $f v_s$; thus, the size of the precursor is $L = \kappa / v_s$. The size of the precursor determines the reflection time, which in turn determines the acceleration time. The mean time for particles to cross the shock from upstream to downstream, $t_{1 \rightarrow 2}$, is determined by equating the mean flux $f(p)L/t_{1 \rightarrow 2}$ with the flux measured at the shock front, $f(p)w/4$, which gives $t_{1 \rightarrow 2} = 4L/w = 4\kappa_1/wv_s$. A similar argument can be advanced to estimate the time for particles to cross the shock in the opposite direction, $t_{2 \rightarrow 1} \simeq 4\kappa_2/wv_2$, but it is more heuristic since there is no gradient behind the shock. The reflection time t_{refl} is simply the sum of these two time scales. With the aid of Equation (4.2), this argument yields (Krymsky et al 1979)

$$t_{\text{acc}} = \frac{3}{\Delta v} \left(\frac{\kappa_1}{v_s} + \frac{\kappa_2}{v_2} \right). \quad (4.5)$$

In general, κ is expected to increase with particle kinetic energy E . A

minimum value of κ is often taken to be that corresponding to a mean free path equal to one Larmor radius $r_L = pc/eB$; the corresponding diffusion coefficient is $\kappa_{\min} = r_L w/3$, which increases approximately linearly with the kinetic energy of the particle. For a relativistic particle of kinetic energy $E_G \equiv E/(1 \text{ GeV}) > 1$, we have $\kappa_{\min} = 1.1 \times 10^{22} E_G (3\mu G/B_0) \text{ cm}^2 \text{ s}^{-1}$. If we assume that the particles spend comparable times on each side of the shock front (as in the models of Falle & Giddings 1987), and we take $\Delta v = 3v_s/4$ in Equation (4.5), the minimum acceleration time is

$$t_{\text{acc, min}} = \frac{8\kappa_{\min, 1}}{v_s^2} = 2.8 \left(\frac{E_G}{v_s^2} \right) \left(\frac{3\mu G}{B_0} \right) \text{ yr.} \quad (4.6)$$

Bell (1978) calculated the diffusion coefficient associated with the growth of the instability due to the streaming of the cosmic rays through the background plasma (Wentzel 1974),

$$\kappa = \frac{4}{3\pi} \frac{r_L \omega}{I(p)}, \quad (4.7)$$

where $(B_0^2/8\pi)I(p)d\ln p$ is the wave energy in fluctuations between wave-numbers k and $k+dk$, where $k = eB_0/pc$. Generally, $I(p)$ decreases with momentum so that κ increases with energy at least as fast as κ_{\min} ; for the quasi-linear assumption underlying Equation (4.7) to be valid, the normalized intensity $I(p)$ must be less than unity and $\kappa > \kappa_{\min}$. Numerical simulations (Zachary 1987, Max et al 1992) suggest that κ is somewhat larger than these simple estimates if the amplitude of the field fluctuations is in the range $0.1B_0 \lesssim \delta B \lesssim B_0$, but with κ scaling with energy approximately as does κ_{\min} . We conclude that the size of a cosmic-ray precursor increases with energy at least as rapidly as E . The maximum energy of the accelerated particles, E_{\max} , and the corresponding precursor size, L_{\max} , are therefore set by the temporal or spatial limitations on the shock.

For an evolving shock such as that associated with a SNR, E_{\max} is set by the age of the shock. In such shocks, particle acceleration is intrinsically time dependent. For a spherical shock expanding as $R \propto t^\eta$ (a Sedov-Taylor blast wave has $\eta = 2/5$), the age is $t = \eta R/v_s$. If the acceleration time is $t_{\text{acc}} = 8\kappa_1/v_s^2 = 8L/v_s$ as in Equation (4.6), then the precursor size corresponding to particles with an acceleration time equal to the age is

$$\frac{L_{\max}}{R} = \frac{\eta}{8} \sim 0.05, \quad (4.8)$$

where the numerical value is for a Sedov-Taylor blast wave. Thus most of the accelerated particles are confined to a relatively thin shell outside the shock. Some of the particles, however, have large excursions

ahead of the shock and may escape—in Bell’s model, the density ahead of the shock varies as $1/(L+x)$, a relatively slow decline. The particles suffer adiabatic expansion losses during the fraction of the time that they are behind the shock, but these losses are generally small compared to the gains so long as the acceleration continues. The maximum energy is given implicitly by $\kappa(E_{\max}) = L_{\max}v_s$; setting the diffusion coefficient equal to κ_{\min} gives an upper bound on the Larmor radius, $r_L(E_{\max}) \lesssim 0.15(v_s/w)R$. The corresponding limit on the maximum energy is $E_{\max} = 5100(B_0/3\mu G)(E_{51}v_{s7}/n_0)^{1/3}$ GeV. Even for a young SNR ($v_{s7} \approx 30$) in a low density region ($n_0 \approx 0.003$) this yields $E_{\max} \approx 10^5$ GeV, well below the energy $\sim 5 \times 10^6$ GeV at which the spectrum of Galactic cosmic rays steepens (Fichtel & Linsley 1986)—a serious problem for the shock acceleration theory of cosmic rays (Lagage & Cesarsky 1983).

The wave generated in a shock with particle acceleration can be described by the wave energy equation derived by Dewar (1970). For Alfvén waves streaming opposite to the flow, this equation is

$$\frac{\partial}{\partial t} W + \frac{\partial}{\partial z} W(v - v_{Ai}) + \frac{1}{2} W \frac{\partial}{\partial z} v = v_{Ai} \frac{\partial}{\partial z} P_{cr} - \text{damping} \quad (4.9)$$

(McKenzie & Völk 1982), where W is the wave energy density and $v_{Ai} = v_A/x_i^{1/2}$ is the Alfvén velocity in the ionized component of the plasma. The term proportional to P_{cr} represents the rate at which the cosmic rays do work on the waves. To estimate the amplitude of the waves ahead of the shock, we work in the shock frame ($\partial/\partial t = 0$), neglect damping, and assume that $v \approx v_s \gg v_{Ai}$. We then find $v_s W \approx v_{Ai} P_{cr}$, so that the wave energy is a small fraction of the cosmic ray energy.

Bell (1978) worked out the amplitude of the waves under the assumption that the amplitude is small. In this quasi-linear case, waves of a given wavenumber k interact only with particles of momentum $p = eB_0/kc$, and the result we found for the wave amplitude is valid differentially, $v_s dW \approx v_{Ai} dP_{cr}$. We express the wave energy in terms of the amplitude $I(p)$ introduced in Equation (4.7), $dW = I(p)(B_0^2/8\pi)d\ln p$. Let ϕ_{cr} be the normalized cosmic ray pressure,

$$P_{cr} \equiv \phi_{cr} \rho_0 v_s^2, \quad (4.10a)$$

so that ϕ_{cr} measures the efficiency of particle acceleration by the shock. For the limiting case of particle acceleration in a strong shock ($f \propto p^{-2}$ for $p < p_u$ and $f \approx 0$ otherwise), we have

$$\frac{dP_{cr}}{d\ln p} = \frac{w/c}{\ln [(p_u/mc) + (1 + p_u^2/m^2 c^2)^{1/2}]} \cdot \phi_{cr} \rho_0 v_s^2 \quad \text{for } \alpha = 2. \quad (4.10b)$$

Approximating the momentum-dependent term, we find that the normalized intensity is

$$I(p) \simeq \frac{2v_s \phi_{\text{cr}}}{v_A x_i^{1/2}} \cdot \frac{(w/w_u)}{\ln(2.718 + 2E_{uG})}, \quad (4.11a)$$

where E_{uG} is the upper limit on the kinetic energy (in GeV) of the cosmic rays. Bell's quasi-linear approximation [$I(p) \lesssim 1$] is then valid for

$$\phi_{\text{cr}} < 9.2 \times 10^{-3} \left(\frac{x_i^{1/2} B_{-6}}{n_0^{1/2} v_{s7}} \right) \ln(2.718 + 2E_{uG}), \quad (4.11b)$$

which is very insensitive to the maximum particle energy E_u . As we shall see below, theory and observation suggest that the efficiency of particle acceleration often violates the limit imposed by quasi-linear theory, so that phenomenological models for wave-particle scattering must be used. As suggested by Völk et al (1984), it seems likely that violation of this condition, corresponding to magnetic field fluctuations with $I(p_u) > 1$, will be accompanied by rapid dissipation of the MHD waves required to sustain the cosmic ray acceleration. In this case, Equation (4.9) will be satisfied by balancing the work done by the cosmic rays against damping, and Equation (4.11a) will not apply.

If the shock is advancing into a partially neutral medium, then the waves that scatter the particles are subject to ion-neutral damping at a rate $\Gamma = n(H^0) \langle \sigma_x v \rangle$, where the charge exchange rate coefficient is $\langle \sigma_x v \rangle \simeq 8.4 \times 10^{-9} T_4^{0.4} \text{ cm}^3 \text{ s}^{-1}$ for $10^2 \text{ K} \lesssim T \lesssim 10^5 \text{ K}$ (Kulsrud & Cesarsky 1971). Bell (1978) has pointed out that this damping becomes important when the fraction of cosmic rays escaping upstream due to the damping is quite small, of order the fraction $\sim (v_s/w)$ escaping downstream. Damping sets an upper limit on the energy of the accelerated particles, since the growth rate of the cosmic ray streaming instability

$$\omega_I = \frac{e\pi^{3/2}}{2\alpha\rho_i^{1/2}c} p f(p) (v_s - v_{Ai}) \propto p^{1-\alpha} \quad (4.12)$$

(Kulsrud & Cesarsky 1971), is a declining function of energy; here ω_I is the growth rate for the wave amplitude, and ρ_i is the density of the ambient ions. Note that this expression for ω_I , which is exact, differs by a numerical factor from the approximate expression derived by Skilling (1975). Re-expressing Bell's (1978) result in terms of the postshock pressure in cosmic rays, $\phi_{\text{cr}} \rho_0 v_s^2$, we find that the maximum energy particles can acquire before losses become important, E_u , is given by

$$E_{uG} \approx 0.49 A^{2/3} \quad \text{for } A \ll 1, \quad (4.13a)$$

$$E_{\text{uG}} \ln(2E_{\text{uG}}) \approx A \quad \text{for } A \gg 1, \quad (4.13\text{b})$$

$$A = 3.0 \times 10^{-3} \frac{v_{s7}^4 \phi_{\text{cr}}}{x_i^{1/2} (1-x_i) n_0^{1/2} T_4^{0.4}}, \quad (4.13\text{c})$$

where we have adopted a spectrum appropriate for a strong shock, $f(p) \propto p^{-2}$; as is the case throughout this review, we have assumed that the abundance of helium is 10% by number. These limits on the particle energy are based on the quasi-linear approximation, which requires that the efficiency of particle acceleration be low (Equation 4.11b); for more efficient shocks, these limits are only rough estimates.

In order for the particle spectrum to extend to relativistic energies, we require $A > 1$, which sets a lower limit on the shock velocity:

$$v_{s7} > 4.3 \left[\frac{x_i^{1/2} (1-x_i) n_0^{1/2}}{\phi_{\text{cr}}} \right]^{1/4} T_4^{0.1} \quad (4.14)$$

(cf McKee & Hollenbach 1980). Any shock in the hot component of the interstellar medium ($n_0 \sim 0.003$, $T \sim 5 \times 10^5$ K) will satisfy Equation (4.14) because the hot medium is so highly ionized, and as a result such shocks can produce high energy cosmic rays. However, in a partially ionized medium (e.g. $n_0 \gtrsim 0.1$, $x_i \lesssim 0.5$, $B_{-6} \sim 3$) only very fast shocks can accelerate particles to relativistic energies: Inserting $x_i \approx 0.5$ and $\phi_{\text{cr}} \sim 0.1$ in this expression for the shock velocity gives $v_{s7} \gtrsim 6n_0^{1/8}$ as the minimum required. Radiative shocks can produce ionizing precursors (Section 2.4.1). If the ionization due to the precursor is incomplete, then ion-neutral damping is likely to be sufficiently effective that the accelerated particles will not reach relativistic energies. On the other hand, if the pre-ionization is complete [$v_{s7} \gtrsim 1.1$ for $T_{e2} = T_{e2}^{\text{eq}}$ according to Shull & McKee (1979)], then the neutral fraction in the precursor is quite small ($[1-x_i] \sim 10^{-3}$) and relativistic particle acceleration is possible. Even in this case, however, the energy of the accelerated particles is quite limited: In a SNR, gas first cools to 10⁴ K at the shell formation time, when $v_{s7} \approx 1.8n_0^{1/7} E_{51}^{1/4}$ km s⁻¹ (Cioffi et al 1988), and according to Equation (4.13) the maximum energy is then (for $\phi_{\text{cr}} \approx 0.1$, $[1-x_i] \approx 10^{-3}$) about $2n_0^{1/14} E_{51}^{2/7}$ GeV. We conclude that shocks that are optically observable, either as nonradiative shocks in a partially neutral medium or as radiative shocks, are generally unable to accelerate particles to extremely relativistic energies.

In principle, interstellar shocks can accelerate dust grains and photons as well as charged particles. Dust grains are generally charged, and their Larmor radii behind a shock are comparable to those of high energy cosmic rays; once they acquire a velocity large compared to that of the

shock, they can be accelerated as efficiently as the cosmic rays (Epstein 1980). However, it is not at all clear how the grains would attain this initial velocity. Shocks propagating in media with substantial concentrations of neutral hydrogen can accelerate Ly α photons (Neufeld & McKee 1988). Since these photons are subject to absorption by dust, this effect is particularly important in regions of low dust content, such as galaxies at high redshift.

4.2.2 COSMIC-RAY MEDIATED SHOCKS Unless some process inhibits the injection of superthermal particles into the shock, particle acceleration will continue until the cosmic rays begin to affect the structure of the shock and regulate their acceleration (Eichler 1979). Shocks in ionized gas are thus expected to be multifluid shocks just as are shocks in weakly ionized gas (Sections 3). As in the latter case, a trace constituent of the plasma (in this case, the cosmic rays) has a sound speed larger than the shock velocity. Energy losses from the shock due to escaping high energy particles may affect the structure, just as radiative losses do in the weakly ionized case. However, there are significant differences as well: In the cosmic ray case, the coupling between the fluids is collisionless and is not fully understood. Furthermore, the cosmic rays are not a single fluid; their energy spectrum extends over many decades, and the size of the cosmic-ray precursor increases with energy.

Most of the calculations of shocks mediated by cosmic rays have focused on steady shocks. This approach is accurate for standing shocks, or for expanding shocks in which damping limits the maximum particle energy (Equation 4.13); for evolving shocks in which the maximum energy is determined by the age of the shock, the steady state assumption is invalid. In the idealized case in which κ is independent of momentum, it is possible to treat the cosmic rays as a fluid coupled to the thermal gas. In this two-fluid approach, the shock jump conditions must be supplemented by an additional parameter, the effective adiabatic index of the downstream gas, γ_{eff} (Achterberg et al 1984). This parameter characterizes the downstream spectrum of the cosmic rays: For $\gamma_{\text{eff}} \simeq 5/3$, the cosmic rays are non-relativistic and/or they make a negligible contribution to the downstream pressure; for $\gamma_{\text{eff}} \simeq 4/3$, relativistic cosmic rays dominate the downstream pressure of the gas. Two-fluid calculations can yield the paradoxical result that cosmic rays can be produced from nothing—the shock can be cosmic-ray dominated even if there are no cosmic rays initially and there is no J-shock to produce them (Drury & Völk 1981). Such a solution is unphysical: It corresponds to putting a finite energy into an infinitesimal number of particles, but since there is an upper limit to the particle energy this cannot occur. On the other hand, when preexisting cosmic rays are present, as

they are in any actual astrophysical system, the two-fluid calculations suggest that a smooth, cosmic-ray dominated shock with no viscous sub-shock—a C-shock—can occur for Mach numbers $M \gtrsim 6$ –12, depending on the value of γ_{eff} . Such shocks put most of their energy into cosmic rays.

In the more realistic case in which κ increases with energy, the high energy particles in a strong shock will see a compression greater than 4, causing the energy density in the cosmic rays to diverge (see Equation 4.4). To avoid this divergence for steady shocks, one must either set an upper limit on the shock Mach number (Heavens 1984) or explicitly allow for the escape of the high energy particles (Drury 1984, Eichler 1984, Krymsky 1984). In the latter, high Mach number case, one must specify two additional parameters: the maximum particle energy E_{max} , which is set by the size of the system (Section 4.2.1), and the rate at which particles are accelerated to E_{max} and are lost from the system. In order to self-consistently calculate γ_{eff} and the energy loss, it is necessary to calculate the spectrum of the cosmic rays (Eichler 1984, Krymsky 1984). In the absence of a preexisting population of cosmic rays, such calculations lead to a J-shock (generally referred to as a “viscous subshock” in the literature) with a cosmic-ray precursor. Monte Carlo simulations by Ellison & Eichler (1984) and by Ellison et al (1990) of a quasi-parallel interplanetary shock and bow shock, respectively, are in reasonably good agreement with observations of the energetic particle spectra. These simulations had sonic Mach numbers $M \leq 10$, but the same technique has shown that the basic structure of a J-shock with a cosmic-ray precursor exists for shocks with Mach numbers up to 170 (Ellison & Reynolds 1991). These simulations had no preexisting cosmic rays; approximate analytic calculations by Berezhko et al (1990) suggest that in the absence of a magnetic field ($M_A = \infty$) J-shocks with Mach numbers $M \gtrsim 10$ disappear if a significant fraction of the upstream pressure is due to preexisting cosmic rays.

Time-dependent calculations of spectra of accelerated particles have been carried out by Bell (1987), Falle & Giddings (1987), and Kang & Jones (1991). These studies confirm the time scale for particle acceleration given by Equation (4.5). Falle & Giddings point out that the shocks evolve on the acceleration time t_{acc} , which is significantly greater than the flow time L/v_s ; here $L = \bar{\kappa}/v_s$ is the size of the cosmic-ray precursor based on the mean diffusion coefficient. Time-dependent shocks thus evolve through a sequence of solutions to the steady-state equations, except that now the energy can be concentrated in extremely relativistic particles without causing a divergence. The results of both sets of calculations show no evidence for a J-shock at Mach numbers $M \gtrsim 10$, in contrast to the steady-state Monte Carlo calculations of Ellison and coworkers. It should be

noted, however, that in the time-dependent calculations the injection rate was treated as a free parameter rather than determined self-consistently.

There are several effects that tend to extend the range of conditions for J-shocks and to decrease the amount of energy going into superthermal particles: First, the waves with which the particles interact have a finite phase velocity; insofar as the waves upstream propagate primarily away from the shock, this reduces the compression of the cosmic rays and softens their spectrum (Bell 1978). Second, these waves may grow to large amplitude and damp, putting their energy into the thermal plasma (McKenzie & Völk 1982). Two-fluid calculations incorporating these effects show that the predicted range of conditions under which J-shocks can exist is substantially increased (Völk et al 1984, Heavens 1984, Ellison & Eichler 1985). In particular, Heavens has shown that if the downstream cosmic rays are isotropic in the fluid frame (moving at v_2) and the upstream cosmic rays are isotropic in the wave frame (moving at velocity $v_s - v_{A1}$), then J-shocks can exist at arbitrarily high sonic Mach numbers M provided the Alfvén Mach number satisfies $M_A < 24.6$. When the cosmic-ray pressure in the precursor is significant, the phase velocity of the Alfvén waves is substantially increased, reaching about 10% of the shock velocity according to the calculations of Fiorito et al (1990); this corresponds to an effective Alfvén Mach number of about 10, which would ensure the existence of a J-shock at arbitrarily large sonic Mach numbers if the calculation of Heavens (1984) applies (see Ellison & Eichler 1985).

The third effect that can reduce the efficiency of particle acceleration is that the cosmic-ray precursor is itself unstable: Sound waves propagating toward the shock are amplified provided the shock velocity is somewhat greater than the local sound speed (Drury 1984; see Section 5.3). Numerical simulations show that the instability leads to the formation of viscous subshocks in the precursor (Drury & Falle 1986), although the simulations of Kang et al (1992) do not indicate that this significantly alters the efficiency of particle acceleration. Because of this instability, it is unlikely that pure C-type shocks can exist; viscous subshocks will always be present to inject particles into the acceleration process. Ryu et al (1993) find that the acoustic instability is accompanied by a secondary Rayleigh-Taylor-like instability (see Section 5.3).

The state of our ignorance of shock structure with particle acceleration can be simply summarized: At present we do not have a clear picture of the structure, nor do we know what fraction of the postshock energy goes into accelerated particles. In many cases the shock will not be steady because the acceleration time scale is so great, and the range of possible unsteady shock structures is enormous. If the shock is steady and there is no population of preexisting superthermal particles, the shock is J-type,

but in the more realistic case in which such a population exists, it is not known under what conditions, if any, a C-type shock is possible. If the shock is propagating into a medium that is not fully ionized, the waves will be subject to ion-neutral damping, which could significantly alter the shock structure (see Section 4.2.3 below). Radiative losses in shocks, which are typically important for $v_s \lesssim 200 \text{ km s}^{-1}$ (Section 2.4), can substantially increase the compression; the effect on the structure of the cosmic-ray precursor is unknown.

The efficiency of particle acceleration is uncertain by an order of magnitude. A phenomenological lower limit on the efficiency can be set if the shock waves of SNRs are the source of cosmic rays: For a supernova rate of one per 30 yr in the Galaxy, at least 3% of the supernova energy must go into cosmic rays (Blandford & Eichler 1987). This figure would be increased if the accelerated particles suffer adiabatic expansion losses, as is likely. Time-dependent models of SNRs (Dorfi 1991, Kang & Jones 1991) indicate that $\sim 10\text{--}30\%$ of the initial explosion energy goes into cosmic ray acceleration. An upper limit on the efficiency for high Mach number shocks in the absence of preexisting cosmic rays is given by the calculation of Ellison & Reynolds (1991), who did not consider the effects of a finite Alfvén velocity or of possible instabilities in the precursor; they find that about 80% of the shock energy goes into superthermal particles. Further observational and theoretical work will be needed to reduce this uncertainty.

4.2.3 OBSERVATIONAL IMPLICATIONS FOR SHOCKS

X-ray observations of SNRs provide dramatic evidence that strong shocks are efficient at heating thermal electrons. On this basis one can conclude that either the shocks have viscous subshocks with collisionless heating of the electrons, or that relativistic particles give substantial energy to the plasma through wave damping. In Section 2.3, we discussed evidence from young supernova remnants that collisionless processes can heat the electrons to at least 20% of the equipartition temperature, corresponding to $\gtrsim 10\%$ of the shock energy. If the electrons are as hot as the ions, this limits the energy in cosmic rays to $\lesssim 80\%$ of the shock energy; if the ions are hotter than the electrons, as is to be expected from observations of shocks in the solar system, then the efficiency is less.

Radio synchrotron emission from SNRs has been interpreted in terms of diffusive shock acceleration by Blandford & Cowie (1982). They show that the compression of cold and warm clouds by radiative shocks can accelerate preexisting cosmic ray electrons to high enough energy to account for the observations of old remnants. Fulbright & Reynolds (1990) have calculated the radio morphology to be expected from SNRs

under the opposite assumption that the ISM is homogeneous; they find that acceleration at quasi-perpendicular shocks gives somewhat better agreement with observation than the standard quasi-parallel acceleration.

Nonradiative shocks in partially neutral gas provide a powerful diagnostic for the structure of collisionless shocks (Section 4.1), and this is true for the cosmic-ray precursor as well. In such shocks, ion-neutral damping severely restricts the energies particles can attain; as we saw from Equation (4.14) particles can reach relativistic energies only if $v_s \gtrsim 600n_0^{1/8} \text{ km s}^{-1}$. For any nonradiative shock in a partially neutral gas, one can show that the upper limit on the particle energy is small enough to ensure that the cosmic-ray precursor is collisionless; i.e. the precursor thickness L is less than the charge exchange length L_{cx} . In Bell's theory, $L = v_s/2\omega_I$, where ω_I is the growth rate of the cosmic ray streaming instability at the shock front. The dominant collisional process in a partially neutral medium is charge exchange, and the distance that the shock moves in one charge exchange time is $L_{\text{cx}} \sim v_s/\Gamma$, where Γ is the ion-neutral damping rate. Hence, $L/L_{\text{cx}} \sim \Gamma/2\omega_I$. But Bell has shown that the damping is important when $\Gamma \simeq (v_s/w)\omega_I$, so that $L/L_{\text{cx}} \sim v_s/2w \ll 1$, and the cosmic-ray precursor is small compared to the collision length. As a result, the gross structure of such a shock is unaffected by particle acceleration: The neutrals penetrate into the shocked plasma before interacting with it. Thermalization of the neutral kinetic energy adds to the energy of thermal plasma behind the shock and decreases the overall efficiency of particle acceleration.

An attempt to directly observe the effects of particle acceleration in an interstellar shock was made by Morfill et al (1984), who suggested that the heating of electrons in the precursor would create an X-ray halo around young SNRs such as Cas A. It now appears that the observed haloes are due to scattering by intervening interstellar dust, however (Mauche & Gorenstein 1989).

Boulares & Cox (1988) have carried out the first extensive study of the temperature and ionization structure of cosmic-ray precursors. They applied their results to three types of shocks seen in the Cygnus Loop SNR (X-ray emitting shocks in a cloudless medium, Balmer-dominated shocks, and radiative shocks), and argued that cosmic-ray-dominated shocks could account for the data at least as well as the standard gas dynamic shocks. Indeed, in the “Spur,” a bright region in the southeastern part of the remnant, Raymond et al (1988) measured a ram pressure of $\sim 1.9 \times 10^{-9} \text{ dyne cm}^{-2}$, almost an order of magnitude greater than the thermal pressure in the X-ray emitting gas or in the optical filaments, and Boulares & Cox argue that the missing pressure is most likely due to cosmic rays. A remarkable consequence of their model is that the X-ray emitting shocks,

which are usually inferred to have $v_s \sim 400 \text{ km s}^{-1}$, must have $v_s > 1000 \text{ km s}^{-1}$, whereas the radiative shocks must have $v_s \sim 250 \text{ km s}^{-1}$ instead of the usual 100 km s^{-1} . They used a two-fluid model for the shock structure. Since such models give C-shocks at high Mach numbers, they assumed that the waves were promptly damped in order to heat the thermal plasma (Völk et al 1984). The two-fluid model has a constant diffusion coefficient κ , so they were unable to model the spatial variation of the heating rate in the precursor; their results show that the temperature and ionization in the precursor depend sensitively on κ , so this is a significant limitation. They suggest that the Balmer-dominated filaments lie in the precursors of the X-ray emitting shocks, but such a model encounters two difficulties. First, their calculations did not include the effects of ion-neutral damping in the partially neutral gas upstream. As shown in Section 4.2.2, such damping should ensure that the precursor is sufficiently thin that the neutrals should reach the shock unimpeded; as a result, the width of the broad component of the Balmer profile should be comparable to the shock velocity. The observed line width in the filament studied by Raymond et al (1983) corresponds to $v_s \simeq 170 \text{ km s}^{-1}$, significantly less than the 750 km s^{-1} required by Boulares & Cox. Second, the temperature inferred from the width of the narrow component is about 35,000 K (Hester et al 1992), significantly less than that required for their X-ray shock model. However, this temperature is too high to be due to photoionization, and it could indicate the presence of a cosmic-ray precursor several times weaker than that in the Boulares & Cox model (Raymond 1991). Heating by such a precursor might also account for the H₂ emission observed by Graham et al (1991).

Boulares & Cox also briefly discuss the role of cosmic rays in the radiative shocks seen in the Cygnus Loop. At present, there is no adequate theory for particle acceleration in such shocks. Compression ratios can reach 100 in radiative shocks, far greater than the maximum of 4 allowed by the standard theory with no escaping particles (see Equation 4.4). They suggest that the acceleration must occur in the radiative portion of the shock, since if it occurred at the shock front the cosmic-ray pressure would prevent the large postshock compressions that are observed. For the case of accelerated electrons, Blandford & Cowie (1982) suggested that acceleration would occur at the collisionless shock front, and that the subsequent compression due to radiative cooling would just adiabatically compress the electrons; for this to be true, the cooling length must be large compared to the diffusion length L . Alternatively, the effects of ion-neutral damping discussed above may provide a different solution: Instead of escaping from the shock in the postshock flow, superthermal particles could be accelerated up to the energy given by Equation (4.13) and then

escape through the preshock gas. In this picture, the shocked gas acts like a mirror that reflects particles upstream. Whatever the final explanation that emerges, Boulares & Cox have demonstrated that SNRs provide a challenging environment in which to test theories of shock acceleration of particles.

5. INSTABILITIES IN SHOCK WAVES

5.1 *Thermal Instability*

Shocks are subject to thermal instabilities due to radiative cooling. Thermal instability results when the cooling time of the gas decreases with decreasing temperature, since then a temperature difference between a parcel of gas and its surroundings will grow with time (Field 1965, Balbus 1986). In shocks, the instability can be either a “local” instability, in which the scale is small enough that the dynamics of the shock are not affected, or a “global” instability, in which variations in the shock velocity play a key role in the instability. McCray et al (1975) suggested that a local thermal instability could account for the filaments seen in SNRs such as the Cygnus Loop. However, Blondin & Cioffi (1989) have shown that the local instability is restricted to wavelengths \lesssim the shock thickness, and that in any case it is masked by the steep density gradient in the cooling postshock gas (see also McKee & Hollenbach 1980).

Shocks can also exhibit a global thermal instability. Consider, for example, a strong shock wave driven by a constant velocity “piston.” If the postshock gas ultimately cools to zero temperature, and no magnetic field is present, then the steady state solution to the fluid equations has the shock front at a constant distance from the piston, and therefore moving with the velocity of the piston; the “standoff” distance of the shock from the piston is proportional to the time it takes for shocked gas to cool to zero temperature. Consider now what happens if the speed of the shock front is perturbed to a larger value. The gas just behind the shock front is compressed by the same compression ratio as in the steady shock solution, but heated to a higher temperature. If the cooling time increases with increasing temperature, then the shocked fluid element will take longer to cool to zero temperature, which in turn means that the shock has to move further away from the piston, which implies that the shock speed must increase over the steady-state value. The details of the instability are clearly connected to the downstream boundary conditions imposed on the shock.

Following observation of this instability in numerical calculations (Langer et al 1981, Gaffet 1983), Chevalier & Imamura (1982) performed a linear stability analysis for a one-dimensional shock driven by a constant velocity piston. For cooling functions $\Lambda \propto \rho^2 T^\alpha$, radiative shocks were

shown to be linearly unstable in a fundamental mode for $\alpha \lesssim 0.4$, and unstable to overtone modes for $\alpha \lesssim 0.8$; the linear analysis was subsequently confirmed by time-dependent numerical calculations (Imamura et al 1984). Bertschinger (1986) extended this work to three dimensions, and showed that transverse modes would be unstable for $\alpha \lesssim 1.0$. Since bremsstrahlung cooling has $\alpha \approx 0.5$, this implies that shocks where free-free emission dominates the cooling will be stable in the fundamental mode, but unstable to overtone and transverse modes. Furthermore, for $10^5 \lesssim T \lesssim 10^7$ K the cooling of interstellar gas in ionization equilibrium is dominated by line emission, and is characterized by $\alpha \approx -(0.5-1)$, so shocks with postshock temperatures in this range may be strongly unstable.

A transverse magnetic field tends to stabilize the flow, since it limits the compression as the gas cools. Both linear stability analysis and numerical simulations of magnetized plane-parallel shocks show that for $\alpha = 0.5$ the shock is stabilized for $M_A < 33$ (Tóth & Draine 1993). For $\alpha = -0.5$, however, the fundamental mode is unstable for $M_A > 7.7$, but the first overtone is unstable for $M_A > 3.7$, and higher overtones are unstable for even lower values of M_A . Thus strong interstellar shocks with $1.5 \lesssim v_{s7} \lesssim 2n_0^{1/7}$ should be strongly unstable.

Innes et al (1987a,b) pointed out that because of this instability, it is unclear to what extent it is meaningful to compare observations of emission from radiative shocks with theoretical models of steady shocks. Innes et al calculated time-dependent shocks driven by constant-pressure pistons (the constant-pressure boundary condition being more appropriate to radiative shocks driven by SNRs) and a realistic cooling function; shocks with $v_s \gtrsim 150$ km s⁻¹ were found to be violently unstable. Instantaneous optical emission spectra (e.g. [OIII]/[OII] line ratios) of such shocks differed appreciably from steady-state calculations. This conclusion remains valid even when the assumption of collisional ionization equilibrium is relaxed (Gaetz et al 1988). Raymond et al (1991) argue that observations of strong CIV absorption indicate the presence of a thermally unstable shock wave in the Vela SNR.

5.2 Ion-Neutral Streaming: Wardle Instability

MHD shocks in gas of low fractional ionization are subject to a novel dynamical instability involving deformation of the magnetic field (Wardle 1990; 1991a,b). The instability operates as follows: Consider a plane-parallel shock with $B_{\parallel} = 0$ and low fractional ionization so that the ion inertia and pressure may be neglected. The net force density on the ions must then be essentially zero. The dominant forces on the ion-electron fluid are the magnetic force $\mathbf{J} \times \mathbf{B}/c = -\nabla B^2/8\pi$ and the drag force due to ion-neutral slip, which is proportional to $\rho^{(n)}\rho^{(i)}(\mathbf{v}^{(n)} - \mathbf{v}^{(i)})$.

Now consider what would happen if the straight magnetic field lines of the plane-parallel steady solution were to be perturbed as in Figure 4. The drag force will now have a component parallel to the local magnetic field that cannot be balanced by the $\mathbf{J} \times \mathbf{B}$ force, and ions will therefore be accelerated along the field lines to collect in the magnetic “valleys.” As a consequence, $\rho^{(i)}$ will increase in the valleys, the drag force (proportional to $\rho^{(i)}$) will increase, and the field lines may be further distorted. Linear stability analysis (Wardle 1990) found C-type MHD shocks with $B_{\parallel} = 0$ to be unstable for $M_A \gtrsim 5$; oblique shocks (in which $B_{\parallel} \neq 0$) behave similarly (Wardle 1991b). The nonlinear development has yet to be investigated, so that it is not yet known to what degree these unstable shocks will differ from the idealized steady-flow solutions that have been studied numerically. The most unstable mode has a wavelength approximately equal to the thickness of the shock transition.

5.3 Cosmic-Ray-Mediated Shocks: Drury Instability

Shocks which are efficient at cosmic-ray acceleration have a postshock cosmic-ray pressure that is an appreciable fraction of the total momentum flux $\rho_0 v_s^2$. As a result, the cosmic-ray pressure gradient in the neighborhood of the shock is dynamically significant. Drury (1984) noted that acoustic

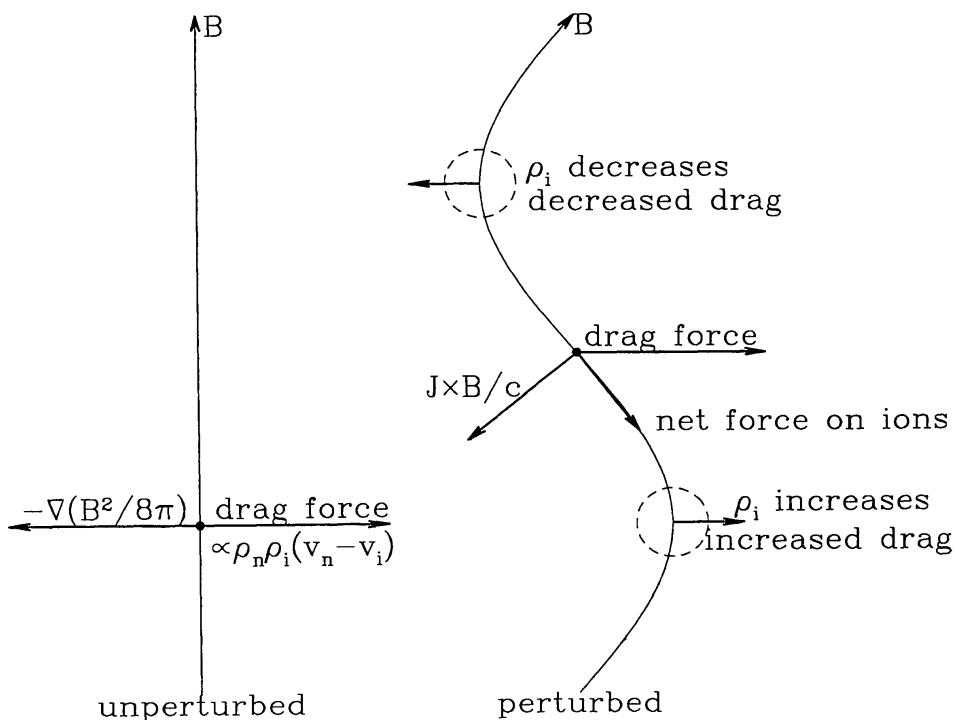


Figure 4 Mechanism for the Wardle instability in two-fluid MHD shock waves.

waves in the preshock medium which are propagating toward the shock may be amplified as they enter the region where the large cosmic-ray pressure gradient is present; waves which (relative to the local gas) are propagating in the direction of decreasing cosmic-ray pressure are damped. To see this, consider a small amplitude sound wave with (local) propagation vector \mathbf{k} and density perturbation $\delta\rho$. The velocity perturbation associated with this wave is $\mathbf{v} = \mathbf{k}c^2\delta\rho/\omega\rho$. The cosmic-ray pressure gradient contributes an acceleration $\mathbf{a} = -(1/\rho)\nabla P_{\text{cr}}$; if we neglect any perturbation in P_{cr} , then $\delta\mathbf{a} = \nabla P_{\text{cr}}\delta\rho/\rho^2$. The rate/volume at which work is done on the wave by the cosmic-ray pressure is second-order: $\delta W = (\rho\delta\mathbf{a})\cdot(\delta\mathbf{v}) = (c^2/\omega)\mathbf{k}\cdot\nabla P_{\text{cr}}(\delta\rho/\rho)^2$; thus if $\mathbf{k}\cdot\nabla P_{\text{cr}} > 0$ then $\delta W > 0$ and the sound wave will be amplified, whereas this effect damps waves with $\mathbf{k}\cdot\nabla P_{\text{cr}} < 0$. A more complete analysis (Drury 1984), taking into account perturbations to P_{cr} , shows that this mechanism only operates for $d\ln\kappa/d\ln\rho > -1$, where κ is the cosmic-ray diffusion coefficient (for $d\ln\kappa/d\ln\rho < -1$ the mechanism tends to amplify waves propagating in the direction of decreasing P_{cr}) and that the instability must overcome damping due to “friction” between the fluid and the cosmic rays.

Numerical simulations of the Drury instability have been carried out by Drury & Falle (1986) and by Kang et al (1992). These simulations show that the instability produces viscous subshocks ahead of the main shock without, however, significantly altering the overall shock structure. Rayleigh-Taylor instabilities arise in the cosmic-ray precursor when the density gradient due to these nonlinear sound waves opposes the cosmic-ray pressure gradient, further complicating the structure of the precursor (Ryu et al 1993).

5.4 *Blast Wave Instabilities*

Decelerating radiative shock waves (e.g. SNRs in the “snowplow” phase) are subject to a rippling instability (Vishniac 1983, Bertschinger 1986, Vishniac & Ryu 1989). The wavelength of maximum instability is of order a few times the thickness of the cold dense shell; the instability is of an overstable nature, and grows in an oscillatory fashion. The dynamical instability of “adiabatic” blast waves has been studied by Ryu & Vishniac (1987), who find such blast waves to be unstable for adiabatic index $\gamma \lesssim 1.2$ (for astrophysical fluids radiative cooling is required for the effective γ to be in this range). Laboratory observations of this instability have recently been reported (Grun et al 1991). Numerical calculations (Mac Low & Norman 1992) show that the overinstability saturates when transverse velocities exceed the sound speed in the shell, consistent with the damping observed at late times in the experiment.

6. DUST IN SHOCKS

6.1 Physical Processes

Many of the heavy elements in the ISM are locked up in dust grains. When a dusty plasma is overtaken by a shock, the grains are subject to destruction by both grain-grain collisions and sputtering. In low-velocity shocks grain destruction is probably dominated by vaporization in grain-grain collisions (Oort & van de Hulst 1946; Spitzer 1968; Jura 1976; Shull 1977, 1978; Seab & Shull 1983; McKee et al 1987). In unmagnetized gas, the grain component will develop a postshock velocity dispersion since the deceleration by gas drag depends on grain sizes, shape, and density. In magnetized gas, a large velocity dispersion will exist due to gyration of charged grains around the field lines, provided the gyroperiod is shorter than the drag time. If the principal force on a grain behind a shock front is due to collisions with gas atoms, it follows on quite general grounds that the probability P_{coll} that a given grain will participate in a grain-grain collision with relative speed $\Delta v \gtrsim v_{\min}$ is $P_{\text{coll}} \approx (\rho_{\text{dust}}/\rho_{\text{gas}}) \ln(v_s/v_{\min})$ where $\rho_{\text{dust}}/\rho_{\text{gas}} \approx 0.006$ is the ratio of total dust mass to gas mass. If cooling and compression of the magnetized gas occurs on a time scale short compared to the gas drag time scale, but long compared to the grain gyroperiod, the charged grains will undergo *betatron* acceleration (Spitzer 1976), significantly enhancing grain destruction; this is particularly effective for large grains.

In shocks with $v_s \gtrsim 100 \text{ km s}^{-1}$, sputtering becomes more important than grain-grain collisions (Barlow 1978, Draine & Salpeter 1979b). The sputtering rates (Draine & Salpeter 1979a) depend both on the gas temperature and on the motion of the grains through the gas, and the degree of sputtering is therefore enhanced by betatron acceleration, if the latter is effective (Cowie 1978). The dependence on the magnetic field strength has been emphasized by McKee et al (1987). Since the postshock compression cannot exceed $2^{1/2} M_A$, the efficacy of betatron acceleration depends upon the Alfvén Mach number M_A , and therefore upon the preshock magnetic field. Stronger magnetic fields (by reducing M_A) can limit the degree of grain destruction in the shock. If the magnetic field is too weak, then betatron acceleration also is ineffective because the gas cooling and compression time becomes short compared to the gyroperiod. Overall, grain destruction fractions of several to several tens of percent are estimated for $v_s \approx 50\text{--}200 \text{ km s}^{-1}$ shocks (Shull 1977, 1978; Draine & Salpeter 1979b; Seab & Shull 1983; McKee et al 1987; Jones et al 1993).

Grain destruction occurs in an extended zone behind the shock transition, so that the immediate postshock gas will still have the original depletion of the preshock medium. Calculation of the resulting line emis-

sion from fast shocks requires careful treatment of both the gradual change in gas-phase abundances, as well as the fact that the material injected into the gas will initially be mainly neutral and not in “ionization equilibrium” with the hot gas. The dynamics of the shocked grains can also affect the spectrum. The dust grains initially contain $\sim 1\%$ of the total energy in the shock; if betatron acceleration is effective, this fraction may be increased. The kinetic energy of the grains is, of course, ultimately dissipated, but this dissipation may occur in cool gas downstream from the shock, thereby affecting the relative strengths of emission from hot and cool postshock regions (McKee et al 1987).

Inelastic collisions of electrons with dust grains can be an important cooling mechanism for the gas: For standard models of the interstellar grain population, this collisional cooling term can exceed atomic cooling processes for temperatures $T \gtrsim 10^6$ K (Ostriker & Silk 1973, Silk & Burke 1974, Draine 1981, Dwek & Arendt 1992). In hot gas, however, the smallest grains (which dominate the surface area) are quickly eroded by sputtering. For shock speeds $300 \lesssim v_s \lesssim 2000$ km s $^{-1}$ approximately 15% of the available energy is radiated before the grains are completely destroyed (Draine 1981). This cooling process can affect the evolution of supernova blast waves in very dense clouds (Draine & Woods 1991).

6.2 *Observational Implications*

Infrared emission from shock-heated dust dominates the spectrum of SNRs such as Cas A (Dwek et al 1987). Infrared observations of remnants provide a powerful tool for studying the morphology of the medium into which the remnants are expanding. A thorough review of the observations of dust in hot (primarily shock-heated) gas has been given recently by Dwek & Arendt (1992).

Shocks are the dominant destruction mechanism for interstellar dust grains, and as such they have a major effect on the gas-phase abundances of a number of elements in the ISM. A number of elements are highly underabundant in interstellar gas (relative to cosmic abundances), and this depletion is believed to be the result of their incorporation into dust grains. Among the abundant elements, Si, Fe, and Ca are typically depleted by factors of 10 or more. Carbon depletions are difficult to measure, but most grain models (e.g. Draine & Lee 1984, Duley et al 1989, Greenberg 1989, Mathis & Whiffen 1989) require C to be depleted by factors of 2–3 (van Dishoeck et al 1992). Oxygen depletion is uncertain.¹ The observed

¹ Ultraviolet absorption line observations suggest O to be “depleted” by a factor ~ 2 (e.g. Cardelli et al 1991). However, observations of the 3.1 μm ice band show little of the oxygen to be in H₂O (see e.g. Table 8 of van Dishoeck et al 1992) and, for solar abundances of Si and O, not more than $\sim 20\%$ of the O could be locked up in silicates. It therefore seems unlikely that more than $\sim 20\%$ of the interstellar oxygen is in grains.

depletions reflect a balance between the creation of dust grains in stellar outflows and the growth of grains in the ISM on the one hand, and the destruction in interstellar shocks on the other. Recent discussions of models of this process can be found in McKee (1989) and Draine (1990).

7. SHOCK CHEMISTRY

7.1 *Hot Chemistry in Molecular Gas*

Shock waves in molecular clouds can have important chemical consequences (see the review by Hartquist et al 1990). Sufficiently fast shocks will destroy the H₂, but slower shocks (which are generally C_{eff} shocks—see Section 3.2) may heat the molecular gas just enough so that a variety of chemical reactions may occur.

Formation of the enigmatic species CH⁺ has been a long-standing problem for the interstellar chemistry of diffuse clouds (Dalgarno 1976). Elitzur & Watson (1978, 1980) proposed that CH⁺ might be produced in shock waves via the endothermic reaction



The shock-production scenario is supported by the observed association of CH⁺ with “hot” H₂ (Lambert & Danks 1986). Single-fluid shocks do not, however, appear to be viable due to insufficient CH⁺ production (Mitchell & Deveau 1983, Mitchell & Watt 1985, Pineau des Forets et al 1986a) or overproduction of OH and rotationally-excited H₂ (Draine 1986b). Two-fluid MHD shocks, however, appeared more promising, and shock models were proposed to explain the CH⁺ observed toward ζ Oph and other stars (Pineau des Forets et al 1986a, Draine 1986b). In these models, ion-neutral streaming helps overcome the energy barrier for reaction (7.1), thereby favoring it relative to neutral-neutral reactions. Recent observational work, however, calls into question the two-fluid shock models for CH⁺ production: Such shocks are predicted to have the CH⁺ formed at a velocity intermediate between the preshock and postshock velocities, but such velocity shifts, though originally reported (Hobbs 1973), have not been confirmed (Lambert et al 1990, Hawkins & Craig 1991). The hypothesis that CH⁺ is formed in shocks remains intriguing, but the published shock models appear to be ruled out. Further theoretical exploration of the conjecture is required.

The CH⁺ ion is subject to dissociative recombination, about 5 orders of magnitude faster than radiative recombination of C⁺ with electrons. Conversion of C⁺ into CH⁺ in a shock can therefore lead to a *decrease* in the ionization fraction (Flower et al 1985): The chemistry thereby directly influences the gas dynamics in the shock.

In addition to CH^+ , diffuse cloud shocks may generate CH and OH in detectable amounts (Draine & Katz 1986a,b). Two-fluid MHD shocks may affect the abundances of sulphur compounds (Pineau des Forets et al 1986b), polyatomic carbon species (Pineau des Forets & Flower 1987, Pineau des Forets et al 1987), and may be influenced by the photo-dissociation of H_2 (Monteiro et al 1988). MHD shocks in dark clouds may also affect the abundances of HOCO^+ (Pineau des Forets et al 1989) and the C/CO ratio (Flower et al 1989).

In both diffuse and dense clouds, OH and H_2O can be generated through the reactions



The first reaction is endothermic and both reactions have significant activation energies, so they do not proceed at significant rates until the temperature exceeds ~ 300 K (Wagner & Graff 1987). They are important because: 1. They remove atomic oxygen, an important reactant; and 2. OH and H_2O are powerful coolants and valuable diagnostics. Strong rotational lines of OH and ^{18}OH have been observed from the OMC-1 region; the emission is believed to originate in shocked gas (Melnick et al 1990, and references therein). Theoretical models predict strong emission in rotational lines of H_2O ; the *ISO* satellite will soon be in a position to test these predictions. Some of the excited rotational levels of H_2O become inverted, producing maser emission; this emission has been attributed to shocks, and the reader is referred to the recent review by Elitzur (1992) for a discussion.

7.2 Dissociative Shocks

For sufficiently high shock speeds, conditions in the shocked gas will lead to destruction of the H_2 , primarily through collisional dissociation. Such shocks are J-type (Section 3.2). The critical shock speed for this depends on the magnetic field and fractional ionization of the preshock gas. For nonmagnetic, single-fluid shocks in gas of density $n_{\text{H}} \gtrsim 10^2 \text{ cm}^{-3}$, shock speeds $v_s \gtrsim 25 \text{ km s}^{-1}$ result in essentially complete destruction of the H_2 (Hollenbach & Shull 1977, Kwan 1977, London et al 1977, Smith 1993b). When two-fluid effects are taken into account, the low fractional ionizations present in dense molecular clouds allow H_2 to survive for shock speeds $v_s \lesssim 45 \text{ km s}^{-1}$ (Chernoff et al 1982, Draine et al 1983, Smith & Brand 1990). Faster shocks will dissociate essentially all of the H_2 , and cooling is then dominated by electronic transitions of atoms and ions. Once the postshock gas cools sufficiently, however, H_2 will begin to reform

both through dissociative attachment ($H^- + H \rightarrow H_2 + e^-$) and on the surfaces of the surviving grains. The H_2 formation process affects the postshock gas in three ways: 1. heat release; 2. creation of a coolant; 3. introduction of a species which can subsequently react to form other molecules, such as OH or H_2O .

Models of such shocks have recently been calculated, including calculations of the atomic and molecular emission spectra (Hollenbach & McKee 1989; Neufeld & Dalgarno 1989a,b). The H_2 emission is dominated by collisional excitation of the low- J rotational lines and formation pumping of the high- J rotational lines and the vibrational lines. [OI]63 μm emission is a good diagnostic for $n_0 v_s$ in such shocks. A number of ionic fine structure lines, such as [NeII]12.8 μm and [SiIII]35 μm are predicted to be much stronger in dissociative shocks than in C_{eff} shocks.

7.3 Confrontation with Observation: The Orion-KL Molecular Outflow

Observations over the past decade have revealed that star formation in dense clouds is frequently accompanied by high-velocity gas flows driven by energetic outflows from young stellar objects (Lada 1985; Reipurth 1989, 1991; Lane 1989; Bally & Lane 1991). These outflows—with velocities ranging from tens to hundreds of $km\ s^{-1}$ —drive shock waves into the surrounding cold cloud material. The shocked gas is observed in several different ways: 1. high velocity “wings” on the low- $J \rightarrow J-1$ CO emission lines; 2. far-infrared emission in rotational lines of OH, and high- $J \rightarrow J-1$ lines of CO; 3. infrared emission lines of H_2 ; 4. in some cases (Herbig-Haro objects), optical emission lines such as $H\alpha$, [OI]6300, and [SII]6731. Some of these outflows—especially the “Herbig-Haro jets” (Reipurth 1989)—are highly collimated. Bow shock models have been proposed to explain the emission from Herbig-Haro objects (e.g. Hartigan et al 1987).

The Kleinmann-Low region in the Orion Molecular Cloud contains a spectacular example of a high-velocity flow. Powerful emission is observed from H_2 , OH, and high- J CO which appears to require dense ($n_H \gtrsim 10^6\ cm^{-3}$) molecular gas at $T \gtrsim 2000\ K$; a shock wave appears to be the only plausible process for producing the hot gas. Two-fluid MHD shock models proposed for this region (Draine & Roberge 1982, Chernoff et al 1982) appeared to be fairly successful in accounting for the observed intensities of emission lines of H_2 , CO, OH, and OI. In these models oxygen chemistry produced significant abundances of OH and H_2O which in turn were important coolants. Line intensity ratios in these two-fluid MHD planar shock models are sensitive to the adopted parameters (shock speed, density, fractional ionization, magnetic field strength and orientation) and

it was therefore expected that maps of OMC-1 would show considerable variations in line intensity ratios across the extended emitting region.

Subsequent observational work has disclosed systematic discrepancies between the models and observations, mainly regarding the relative intensities of the infrared lines of H₂ (Brand et al 1988, 1989); particularly striking is the observational result that in OMC-1 the H₂ line ratios appear to be independent of position! Since the planar MHD shocks appeared to be disfavored, it was proposed that the emission might be due to non-magnetic shocks with only molecular hydrogen cooling: Such shocks do in fact provide a better fit to the overall intensity pattern of the H₂ vibration-rotation lines (Brand et al 1988, Chang & Martin 1991). For shock speeds in the range 10–25 km s⁻¹ the relative intensities of the different lines would be almost independent of the shock speed, since in such a shock appreciable line emission only occurs after the gas temperature has dropped to the point where collisional dissociation ceases to be important.

Unfortunately, cooling due to CO, OH, and H₂O is by no means negligible, and inclusion of these cooling process changes the predicted line intensity ratios, destroying the agreement between the nonmagnetic models and the observations. Furthermore, we have independent reasons for believing that magnetic fields are present, and these fields should affect structure along the lines envisioned by the MHD models. The agreement between observed line intensities and the predictions for pure-H₂ non-magnetic shocks must apparently be regarded as fortuitous.

How then to understand the apparent constancy of H₂ line ratios in the KL region? M. D. Smith et al (1991) proposed that bow shocks might offer the solution. Assuming 1. a paraboloidal bow shock with bow velocity v_b , 2. each section of the bow shock radiates like a plane-parallel radiative shock with shock speed $v_b \cos \theta$ (where θ is the angle between the normal to the bow shock surface and the flow direction), and 3. negligible H₂ emission for $v_b \cos \theta > v_{\text{diss}}$ (where v_{diss} is the shock speed above which H₂ is fully dissociated), then the H₂ emission line ratios, after summing over one bow shock, would be *independent* of the bow velocity v_b provided $v_b > v_{\text{diss}}$. Furthermore, with the H₂O abundance $x(\text{H}_2\text{O})$ treated as a free parameter, they found that the observed H₂ relative line strengths could be reproduced using a reasonable value of $x(\text{H}_2\text{O}) \approx 3 \pm 2 \times 10^{-4}$. For this picture to account for constancy of the H₂ line ratios [which have been mapped with apertures as small as 5" (Brand et al 1989)], it is necessary for the clumps responsible for the bow shocks to be $\lesssim 1"$ in diameter. This in turn seems to imply that hundreds of clumps must be present! Note that in general bow shocks could arise either from fast-moving clumps plowing

into ambient material, or a fast neutral “wind” flowing around dense stationary clumps; in the case of OMC-1 the fact that H₂ line intensities peak near zero velocity seems to favor the fast-moving clump scenario. It is intriguing to note the faint “fingers” of H₂ emission extending radially from the center of the K-L region (Lane 1989): Could these be wakes behind fast-moving clumps?

Smith (1991) has compared the predictions of planar shocks and bow shocks for OMC-1, concluding that the line ratios favor the bow shock picture. However, bow shocks have difficulty in accounting for the large velocity widths observed for some lines, unless uncomfortably large magnetic fields are invoked in order to raise the breakdown velocity to $v_{\text{diss}} \gtrsim 100 \text{ km s}^{-1}$. The nature of this outflow remains a puzzle!

8. FUTURE DIRECTIONS

The theory of interstellar shock waves is a rich subject, and there are many unresolved issues demanding further investigation. Most of these questions are associated with the breakdown of the assumption of an ideal, single-component fluid, an assumption that underlies most of astrophysical fluid dynamics. In this article we have focused on theory, but observational studies will play a crucial role in resolving many of these issues.

The theory of MHD shocks (Section 2) is still incomplete, as the physical relevance of intermediate shocks remains controversial: It has been demonstrated that such shocks can occur in principle when deviations from ideal MHD are considered, but the conditions under which this is relevant for interstellar shocks remain to be determined.

Collisionless shocks involve a number of puzzles. Of greatest practical importance is the question of collisionless heating of electrons by hot ions (Section 2.3.2). Observations indicate that significant collisionless heating takes place under some circumstances, but existing theory is unable to predict the collisionless heating rate nor how much heating takes place. Since the electrons are involved in nearly all the emission processes, this means that we are unable to predict accurately the emission spectrum of collisionless shock waves.

Collisional shock waves also present a number of problems for future work. The cross sections for many fundamental inelastic and reactive processes (e.g. collisional excitation of H₂ by H) are uncertain, making it impossible to accurately model shocks in which these processes are important, either for the shock structure or as diagnostics. Fast multifluid shocks in molecular gas will “break down” when ion-neutral streaming velocities are large enough to cause rapid molecular dissociation and ionization (Section 3.6). Detailed modeling of such shocks requires knowl-

edge of various inelastic cross sections; deviations from Maxwellian velocity distributions may affect rates for dissociation and ionization processes (Hollenbach & McKee 1989). Multifluid shocks in media of low fractional ionization under some circumstances may be unstable to the Wardle instability (Section 5.2), but the nonlinear development of this instability is not yet known. Charged dust grains are likely to be dynamically important when the fractional ionization is low (Section 3.4), since the grains couple both to the plasma (via the Lorentz force) and to the neutral gas (via collisions). A detailed examination is needed to clarify the role of dust grains in multifluid shocks.

Interstellar shocks are thought to be able to accelerate cosmic rays, and this raises a number of fascinating problems involving both the acceleration of cosmic rays and the dynamical effects that cosmic rays may have on shocks (Section 4.2). Some studies suggest that shocks will be extremely efficient at cosmic ray acceleration, with most of the available energy going into cosmic ray acceleration. We have seen above, however, that this can only happen when the MHD waves needed to resonantly scatter the cosmic rays become highly nonlinear. The time-dependence of real astrophysical shocks, the importance of injection of particles into the low energy end of the nonthermal particle distribution, the energy-dependence of the effective diffusion coefficient for cosmic rays near the shock front, and instabilities connected with the cosmic rays (Section 5.3) make modeling these shocks extremely challenging; existing studies have generally been forced to oversimplify at least some aspects of the problem.

ACKNOWLEDGMENTS

We thank J. Arons, P. Cargill, D. Chernoff, D. Eichler, D. Ellison, H. Kang, R. Kulsrud, M. Mac Low, K. Papadopoulos, D. Ryu, L. Spitzer, Jr., and E. Zweibel for helpful discussions. This research was supported in part by NSF grants AST-9017082 and AST-8918573.

Literature Cited

- Achterberg, A., Blandford, R. D., Periwal, V. 1984. *Astron. Astrophys.* 132: 97–104
- Alfvén, H. 1954. *On the Origin of the Solar System*. London: Oxford at the Clarendon
- Asvarov, A. I., Dogiel, V. A., Guseinov, O. H., Kasumov, F. K. 1990. *Astron. Astrophys.* 229: 196–200
- Axford, W. I., Leer, E., Skadron, G. 1977. *Proc. 15th Int. Cosmic Ray Conf. (Plovdiv)* 11: 132
- Bagena, F., Belcher, J. W., Sittler, E. C., Lepping, R. P. 1987. *J. Geophys. Res.* 92: 8603–12
- Balbus, S. A. 1986. *Ap. J.* 303: L79–82
- Bally, J., Lane, A. P. 1991. In *The Physics of Star Formation and Early Stellar Evolution*, ed. C. J. Lada, N. D. Kylafis, pp. 471–95. Dordrecht: Reidel
- Barlow, M. J. 1978. *MNRAS* 183: 367–95
- Bell, A. R. 1978. *MNRAS* 182: 147–56
- Bell, A. R. 1987. *MNRAS* 225: 615–26
- Berezko, E. G., Krymsky, G. F., Turpanov,

- A. A. 1990. *Proc. 21st Int. Cosmic Ray Conf.* (Adelaide) 4: 101–4
- Bertschinger, E. 1986. *Ap. J.* 304: 154–77
- Binette, L., Dopita, M. A., Tuohy, I. R. 1985. *Ap. J.* 297: 476–91
- Blandford, R. D., Cowie, L. L. 1982. *Ap. J.* 260: 625–34
- Blandford, R. D., Eichler, D. 1987. *Phys. Rep.* 154: 1–75
- Blandford, R. D., Ostriker, J. P. 1978. *Ap. J. Lett.* 221: L29–32
- Blondin, J. M., Cioffi, D. F. 1989. *Ap. J.* 345: 853–61
- Borkowski, K. J., Shull, J. M., McKee, C. F. 1989. *Ap. J.* 336: 979–98
- Borkowski, K. J., Shull, J. M. 1990. *Ap. J.* 348: 169–85
- Boulares, A., Cox, D. P. 1988. *Ap. J.* 333: 198–218
- Brand, P. W. J. L., Moorhouse, A., Burton, M. G., Geballe, T. R., Bird, M., Wade, R. 1988. *Ap. J. Lett.* 334: L103–6
- Brand, P. W. J. L., Toner, M. P., Geballe, T. R., Webster, A. S. 1989. *MNRAS* 237: 1009–18
- Bychkov, K. V., Lebedev, V. S. 1979. *Astron. Astrophys.* 80: 167–69
- Canosa, A., Rowe, B. R., Mitchell, J. B. A., Gomet, J. C., Rebrion, C. 1991. *Astron. Astrophys.* 248: L19–21
- Cardelli, J. A., Savage, B. D., Bruhweiler, F. C., Smith, A. M., Ebbets, D. C., et al 1991. *Ap. J. Lett.* 377: L57–60
- Cargill, P. J. 1991. *Adv. Space Res.* 11(9): 209–18
- Cargill, P. J., Papadopoulos, K. 1988. *Ap. J. Lett.* 329: L29–32
- Chang, C. A., Martin, P. G. 1991. *Ap. J.* 378: 202–13
- Chernoff, D. F. 1985. PhD thesis. Univ. Calif., Berkeley
- Chernoff, D. F. 1987. *Ap. J.* 312: 143–69
- Chernoff, D. F., Hollenbach, D. J., McKee, C. F. 1982. *Ap. J. Lett.* 259: L97–102
- Chernoff, D. F., McKee, C. F. 1990. In *Molecular Astrophysics*, ed. T. W. Hartquist, pp. 360–73. Cambridge: Cambridge Univ. Press
- Chevalier, R. A., Imamura, J. N. 1982. *Ap. J.* 261: 543–49
- Chevalier, R. A., Kirshner, R. P., Raymond, J. C. 1980. *Ap. J.* 235: 186–95
- Chevalier, R. A., Raymond, J. C. 1978. *Ap. J. Lett.* 225: L27–30
- Cioffi, D. F., McKee, C. F., Bertschinger, E. 1988. *Ap. J.* 334: 252–65
- Cowie, L. L. 1978. *Ap. J.* 225: 887–92
- Cowie, L. L., Laurent, C., Vidal-Madjar, A., York, D. G. 1979. *Ap. J. Lett.* 229: L81–85
- Cox, D. P. 1972. *Ap. J.* 178: 143–57
- Cox, D. P., Raymond, J. C. 1985. *Ap. J.* 298: 651–59
- Curiel, S. C. 1992. PhD thesis. Univ. Nacional Autonoma de Mexico
- Dalgarno, A., 1976. In *Atomic Processes and Applications*, ed. P. G. Burke, B. L. Moiseiwitsch, pp. 110–32. Amsterdam: North-Holland
- Dewangan, D. P., Flower, D. R., Alexander, M. H. 1987. *MNRAS* 226: 505–12
- Dewar, R. L. 1970. *Phys. Fluids* 13: 2710–20
- Dopita, M. A., Binette, L. 1983. In *Supernova Remnants and Their X-ray Emission*, ed. J. Danziger, P. Gorenstein, pp. 221–30. Dordrecht: Reidel
- Dorf, E. A. 1991. *Astron. Astrophys.* 251: 597–610
- Dove, J. E., Mandy, M. E. 1986. *Ap. J. Lett.* 311: L93–96
- Dove, J. E., Rusk, A. C. M., Cribb, P. H., Martin, P. G. 1987. *Ap. J.* 318: 379–91
- Draine, B. T. 1980. *Ap. J.* 241: 1021–38 (erratum: 246: 1045)
- Draine, B. T. 1981. *Ap. J.* 245: 880–90
- Draine, B. T. 1986a. *MNRAS* 220: 133–48
- Draine, B. T. 1986b. *Ap. J.* 310: 408–18
- Draine, B. T. 1990. In *The Evolution of the Interstellar Medium*, ed. L. Blitz, pp. 193–205. San Francisco: Astron. Soc. Pac.
- Draine, B. T., Katz, N. 1986a. *Ap. J.* 306: 655–66
- Draine, B. T., Katz, N. 1986b. *Ap. J.* 310: 392–407
- Draine, B. T., Lee, H. M. 1984. *Ap. J.* 285: 89–108
- Draine, B. T., McKee, C. F. 1993. In preparation
- Draine, B. T., Roberge, W. G. 1982. *Ap. J. Lett.* 259: L91–96
- Draine, B. T., Roberge, W. G., Dalgarno, A. 1983. *Ap. J.* 264: 485–507
- Draine, B. T., Salpeter, E. E. 1979a. *Ap. J.* 231: 77–94
- Draine, B. T., Salpeter, E. E. 1979b. *Ap. J.* 231: 438–55
- Draine, B. T., Woods, D. T. 1991. *Ap. J.* 383: 621–38
- Drury, L. O'C. 1984. *Adv. Space Res.* 4(2–3): 185–91
- Drury, L. O'C., Falle, S. A. E. G. 1986. *MNRAS* 223: 353–76
- Drury, L. O'C., Völk, H. J. 1981. *Ap. J.* 248: 344–51
- Duley, W. W., Jones, A. P., Williams, D. A. 1989. *MNRAS* 236: 709–25
- Dwek, E., Arendt, R. G. 1992. *Annu. Rev. Astron. Astrophys.* 30: 11–50
- Dwek, E., Dinerstein, H. L., Gillett, F. C., Hauser, M. G., Rice, W. L. 1987. *Ap. J.* 315: 571–79
- Eichler, D. 1979. *Ap. J.* 229: 419–23
- Eichler, D. 1984. *Ap. J.* 277: 429–34
- Elitzur, M. 1992. *Annu. Rev. Astron. Astrophys.* 30: 75–112

- Elitzur, M., Watson, W. D. 1978. *Ap. J. Lett.* 222: L141–44 (erratum: 226: L157)
- Elitzur, M., Watson, W. D. 1980. *Ap. J.* 236: 172–81
- Ellison, D. C., Eichler, D. 1984. *Ap. J.* 286: 691–701
- Ellison, D. C., Eichler, D. 1985. *Phys. Rev. Lett.* 55: 2735–38
- Ellison, D. C., Möbius, E., Paschmann, G. 1990. *Ap. J.* 352: 376–94
- Ellison, D. C., Reynolds, S. P. 1991. *Ap. J.* 382: 242–54
- Epstein, R. 1980. *MNRAS* 193: 723–29
- Falle, S. A. E. G., Giddings, J. R. 1987. *MNRAS* 225: 399–423
- Fermi, E. 1949. *Phys. Rev.* 75: 1169–74
- Fesen, R. A., Blair, W. P., Kirshner, R. P. 1982. *Ap. J.* 262: 171–88
- Fesen, R. A., Blair, W. P., Kirshner, R. P. 1985. *Ap. J.* 292: 29–48
- Fichtel, C. E., Linsley, J. 1986. *Ap. J.* 300: 474–87
- Field, G. B. 1965. *Ap. J.* 142: 531–67
- Field, G. B., Rather, J. D. G., Aannestad, P. A., Orszag, S. A. 1968. *Ap. J.* 151: 953–75
- Fiorito, R. B., Eichler, D., Ellison, D. C. 1990. *Ap. J.* 364: 582–89
- Flower, D. R., Heck, L., Pineau des Forêts, G. 1989. *MNRAS* 239: 741–50
- Flower, D. R., Launay, J.-M. 1985. *MNRAS* 214: 271–77
- Flower, D. R., Pineau des Forêts, G., Hartquist, T. W. 1985. *MNRAS* 216: 775–94
- Formisano, V., Galeev, A. A., Sagdeev, R. Z. 1982. *Planet. Space Sci.* 30: 491–97
- Fulbright, M. S., Reynolds, S. P. 1990. *Ap. J.* 357: 591–601
- Gaetz, T. J., Edgar, R. J., Chevalier, R. A. 1988. *Ap. J.* 329: 927–42
- Gaffet, B. 1983. *Ap. J.* 273: 267–79
- Gosling, J. T., Thomsen, M. F., Bame, S. J. 1989. *J. Geophys. Res.* 94: 10,027–37
- Graham, J. R., Wright, G. S., Hester, J. J., Longmore, A. J. 1991. *Astron. J.* 101: 175–84
- Graham, J. R., Wright, G. S., Longmore, A. J. 1987. *Ap. J.* 313: 847–52
- Graham, J. R., Wright, G. S., Longmore, A. J. 1990. *Ap. J.* 352: 172–83
- Greenberg, J. M. 1989. In *Evolution of Interstellar Dust and Related Topics*, ed. A. Bonnetti, J. M. Greenberg, S. Aiello, pp. 7–52. Amsterdam: North-Holland
- Grun, J., Stamper, J., Manka, C., Resnick, J., Burris, R., et al. 1991. *Phys. Rev. Lett.* 66: 2738–41
- Hamilton, A. J. S., Sarazin, C. L., Szymkowiak, A. E. 1986. *Ap. J.* 300: 713–21
- Hartigan, P., Curiel, S., Raymond, J. 1989. *Ap. J. Lett.* 347: L31–34
- Hartigan, P., Raymond, J., Hartmann, L. 1987. *Ap. J.* 316: 323–48
- Hartquist, T. W., Flower, D. R., Pineau des Forêts, G. 1990. In *Molecular Astrophysics*, ed. T. W. Hartquist, pp. 99–112. Cambridge: Cambridge Univ. Press
- Havnes, O., Hartquist, T. W., Philipp, W. 1987. In *Physical Processes in Interstellar Clouds*, ed. G. E. Morfill, M. Scholer, pp. 389–412. Dordrecht: Reidel
- Hawkins, I., Craig, N. 1991. *Ap. J.* 375: 642–51
- Heavens, A. F. 1984. *MNRAS* 210: 813–27
- Heiles, C., Goodman, A. A., McKee, C. F., Zweibel, E. G. 1992. In *Protostars and Planets III*, ed. E. H. Levy, J. I. Lunine, M. S. Matthews. Tucson: Univ. Ariz. Press. In press
- Hester, J. J., Parker, R. A. R., Dufour, R. J. 1983. *Ap. J.* 273: 219–42
- Hester, J. J., Raymond, J. C., Blair, W. P. 1993. *Ap. J.* Submitted
- Hobbs, L. M. 1973. *Ap. J.* 180: L79–82
- Hollenbach, D. J., Chernoff, D. F. McKee, C. F. 1989. In *Infrared Spectroscopy in Astronomy*, ed. B. H. Kaldeich, pp. 245–58. Noordwijk: ESA
- Hollenbach, D. J., McKee, C. F. 1979. *Ap. J. Suppl.* 41: 555–92
- Hollenbach, D. J., McKee, C. F. 1989. *Ap. J.* 342: 306–36
- Hollenbach, D. J., Shull, J. M. 1977. *Ap. J.* 216: 419–26
- Hughes, J. P. 1991. In *Supernovae*, ed. S. E. Woosley, pp. 661–70. New York: Springer-Verlag
- Imamura, J. N., Wolff, M. T., Durisen, R. H. 1984. *Ap. J.* 276: 667–76
- Innes, D. E., Giddings, J. R., Falle, S. A. E. G. 1987a. *MNRAS* 226: 67–93
- Innes, D. E., Giddings, J. R., Falle, S. A. E. G. 1987b. *MNRAS* 227: 1021–53
- Jokipii, J. R. 1987. *Ap. J.* 313: 842–46
- Jones, A., P., Tielens, A. G. G. M., Hollenbach, D. J., McKee, C. F. 1993. In preparation
- Jones, F. C., Ellison, D. C. 1991. *Space Sci. Rev.* 58: 259–346
- Jura, M. 1976. *Ap. J.* 206: 691–98
- Kang, H., Jones, T. W. 1991. *MNRAS* 249: 439–51
- Kang, H., Jones, T. W., Ryu, D. 1992. *Ap. J.* 385: 193–204
- Kantrowitz, A., Petschek, H. E. 1966. In *Plasma Physics in Theory and Application*, ed. W. B. Kunkel, pp. 147–206. New York: McGraw-Hill
- Kennel, C. F., Blandford, R. D., Wu, C. C. 1990. *Phys. Fluids* B2: 253–69
- Kivelson, M. G., Kennel, C. F., McPherron, R. L., Russell, C. T., Southwood, D. J. et al. 1991. *Science* 253: 1518–22
- Krymsky, G. F. 1977. *Dokl. Akad. Nauk SSSR* 234: 1306–8

- Krymsky, G. F. 1984. *Adv. Space Res.* 4(2–3): 175–84
- Krymsky, G. F., Kuzmin, A. I., Petukhov, S. I., Turpanov, A. A. 1979. *Proc. 16th Int. Cosmic Ray Conf. (Kyoto)* 2: 39
- Kulsrud, R., Cesarsky, C. J. 1971. *Astrophys. Lett.* 8: 189–91
- Kwan, J. 1977. *Ap. J.* 216: 713–23
- Lacey, C. G. 1988. *Ap. J.* 326: 769–78
- Lada, C. J. 1985. *Annu. Rev. Astron. Astrophys.* 23: 267–317
- Lagage, P. O., Cesarsky, C. J. 1983. *Astron. Astrophys.* 125: 249–57
- Lambert, D. L., Danks, A. C. 1986. *Ap. J.* 303: 401–15
- Lambert, D. L., Sheffer, Y., Crane, P. 1990. *Ap. J. Lett.* 359: L19–22
- Landau, L. D., Lifshitz, E. M. 1959. *Fluid Mechanics*. Oxford: Pergamon
- Landau, L. D., Lifshitz, E. M., Pitaevskii 1984. *Electrodynamics of Continuous Media*. Oxford: Pergamon
- Lane A. 1989. In *ESO Workshop on Low Mass Star Formation and Pre-Main-Sequence Objects*, ed. B. Reipurth, pp. 331–348. Garching: ESO
- Langer, S., Chanmugam, G., Shaviv, G. 1981. *Ap. J. Lett.* 245: L23–26
- Levinson, A. 1992. *Ap. J.* 401: 73–80
- Liberman, M. A., Velikovich, A. L. 1986. *Physics of Shock Waves in Gases and Plasmas*. Berlin: Springer-Verlag
- London, R., McCray, R., Chu, S.-I. 1977. *Ap. J.* 217: 442–47
- Mac Low, M. M., Norman, M. L. 1993. *Ap. J.* 407: 207–18
- Mandy, M. E., Martin, P. G. 1992. *J. Chem. Phys.* 97: 265–69
- Mathis, J. S., Whiffen, G. 1989. *Ap. J.* 341: 808–22
- Mauche, C. W., Gorenstein, P. 1989. *Ap. J.* 336: 843–53
- Max, C., Arons, J., Zachary, A. 1992. Preprint
- McCrory, R., Stein, R. F., Kafatos, M. 1975. *Ap. J.* 196: 565–70
- McKee, C. F. 1974. *Ap. J.* 188: 335–39
- McKee, C. F. 1989. In *Interstellar Dust*, ed. L. J. Allamandola, A. G. G. M. Tielens, pp. 431–43. Dordrecht: Kluwer
- McKee, C. F., Chernoff, D. F., Hollenbach, D. J. 1984. In *Galactic and Extragalactic Infrared Spectroscopy*, ed. M. F. Kessler, J. P. Phillips, pp. 103–31. Dordrecht: Reidel
- McKee, C. F., Draine, B. T. 1991. *Science* 252: 397–403
- McKee, C. F., Hollenbach, D. J. 1980. *Annu. Rev. Astron. Astrophys.* 18: 219–62
- McKee, C. F., Hollenbach, D. J., Seab, C. G., Tielens, A. G. G. M. 1987. *Ap. J.* 318: 674–701
- McKenzie, J. F., Völk, H. J. 1982. *Astron. Astrophys.* 116: 191–200
- Melnick, G. J., Stacey, G. J., Genzel, R., Lugten, J. B., Poglitsch, A. 1990. *Ap. J.* 348: 161–68
- Mitchell, G. F., Deveau, T. J. 1983. *Ap. J.* 266: 646–61
- Mitchell, G. F., Watt, G. D. 1985. *Astron. Astrophys.* 151: 121–30
- Monteiro, T. S., Flower, D. R., Pineau des Forêts, G., Roueff, E. 1988. *MNRAS* 234: 863–72
- Morfill, G. E., Drury, L. O'C., Aschenbach, B. 1984. *Nature* 311: 358–59
- Moses, S. L., Coroniti, F. V., Kennel, C. F., Scarf, F. L. 1985. *Geophys. Res. Lett.* 12: 609–12
- Mullan, D. J. 1971. *MNRAS* 153: 145–70
- Neufeld, D. A., Dalgarno, A. 1989a. *Ap. J.* 340: 869–93
- Neufeld, D. A., Dalgarno, A. 1989b. *Ap. J.* 344: 251–64
- Neufeld, D., McKee, C. F. 1988. *Ap. J. Lett.* 331: L87–90
- Newell, P. T. 1985. *Rev. Geophys.* 23: 93–104
- Ohtani, H. 1980. *Publ. Astron. Soc. Jpn.* 32: 11–31
- Oort, J. H., van de Hulst, H. C. 1946. *Bull. Astron. Inst. Neth.* 10: 187–204
- Ostriker, J. P., McKee, C. F. 1988. *Rev. Mod. Phys.* 60: 1–68
- Ostriker, J. P., Silk, J. 1973. *Ap. J. Lett.* 184: L113–15
- Palma, A., Green, S., DeFrees, D. J., McLean, A. D. 1988. *Ap. J. Suppl.* 68: 287–318
- Papadopoulos, K. 1992. *Geophys. Res. Letts.* 19: 605–8
- Parker, E. N. 1961. *J. Nucl. Energy* C2: 146
- Pesses, M. E. 1981. *J. Geophys. Res.* 86: 150–52
- Pilipp, W., Hartquist, T. W., Havnes, O. 1990. *MNRAS* 243: 685–91
- Pineau des Forêts, G., Flower, D. R. 1987. *MNRAS* 228: 1P–4P
- Pineau des Forêts, G., Flower, D. R., Hartquist, T. W., Dalgarno, A. 1986a. *MNRAS* 220: 801–24
- Pineau des Forêts, G., Flower, D. R., Hartquist, T. W., Millar, T. J. 1987. *MNRAS* 227: 993–1011
- Pineau des Forêts, G., Roueff, E., Flower, D. R. 1986b. *MNRAS* 223: 743–56
- Pineau des Forêts, G., Roueff, E., Flower, D. R. 1989. *J. Chem. Soc. Faraday Trans.* 85: 1665–71
- Pravdo S. H., Smith, B. W. 1979. *Ap. J. Lett.* 234: L195–98
- Priest, E. R. 1982. *Solar Magnetohydrodynamics*. Dordrecht: Reidel
- Quest, K. B. 1988. *J. Geophys. Res.* 93: 9649–80
- Raymond, J. C. 1991. *Publ. Astron. Soc. Pac.* 103: 781–86

- Raymond, J. C., Blair, W. P., Fesen, R. A., Gull, T. R. 1983. *Ap. J.* 275: 636–44
- Raymond, J. C., Hester, J. J., Cox, D., Blair, W. P., Fesen, R. A., Gull, T. R. 1988. *Ap. J.* 324: 869–92
- Raymond, J. C., Wallerstein, G., Balick, B. 1991. *Ap. J.* 383: 226–32
- Reipurth, B. 1989. In *ESO Workshop on Low Mass Star Formation and Pre-Main-Sequence Objects*, ed. B. Reipurth, pp. 247–79. Garching: ESO
- Reipurth, B. 1991. In *The Physics of Star Formation and Early Stellar Evolution*, ed. C. J. Lada, N. D. Kylafis, pp. 497–538. Dordrecht: Reidel
- Roberge, W. G., Draine, B. T. 1990. *Ap. J.* 350: 700–21
- Roikhvarger, Z. B., Syrovatskii, S. I. 1979. *Zh. Eksp. Teor. Fiz.* 66: 1338–42
- Romanik, C. J. 1988. *Ap. J.* 330: 1022–35
- Romanik, C. J. 1993. *Ap. J.* In press
- Ryu, D., Kang, H., Jones, T. W. 1993. *Ap. J.* 405: 199–206
- Ryu, D., Vishniac, E. T. 1987. *Ap. J.* 313: 820–41
- Schinke, R., Engel, V., Buck, U., Meyer, H., Diercksen, G. H. F. 1985. *Ap. J.* 299: 939–46
- Schwartz, S. J., Thomsen, M. F., Bame, S. J., Stansberry, J. 1988. *J. Geophys. Res.* 93: 12,923–31
- Scudder, J. D., Mangeney, A., Lacombe, C., Harvey, C. C., Wu, C. S., Anderson, R. R. 1986. *J. Geophys. Res.* 91: 11,075–97
- Seab, C. G., Shull, J. M. 1983. *Ap. J.* 275: 652–60
- Shull, J. M. 1977. *Ap. J.* 215: 805–11
- Shull, J. M. 1978. *Ap. J.* 226: 858–62
- Shull, J. M., Draine, B. T. 1987. In *Interstellar Processes*, ed. D. J. Hollenbach, H. A. Thronson Jr., pp. 283–319. Dordrecht: Reidel
- Shull, J. M., McKee, C. F. 1979. *Ap. J.* 227: 131–49
- Silk, J., Burke, J. R. 1974. *Ap. J.* 190: 11–17
- Skilling, J. 1975. *MNRAS* 173: 255–69
- Smith, A., Davelaar, J., Peacock, A., Taylor, B. G., Morini, M., Robba, N. R. 1988. *Ap. J.* 325: 288–95
- Smith, M. D. 1991. *MNRAS* 253: 175–83
- Smith, M. D. 1992. *Ap. J.* 390: 447–53
- Smith, M. D. 1993a. *MNRAS*. Submitted
- Smith, M. D. 1993b. *Astron. Astrophys.* Submitted
- Smith, M. D., Brand, P. W. J. L. 1990. *MNRAS* 242: 495–504 (erratum: 244: 384)
- Smith, M. D., Brand, P. W. J. L., Moorhouse, A. 1991. *MNRAS* 248: 451–56
- Smith, R. C., Kirshner, R. P., Blair, W. P., Winkler, P. F. 1991. *Ap. J.* 375: 652–62
- Spicer, D. S., Clark, R. W., Maran, S. P. 1990. *Ap. J.* 356: 549–571
- Spitzer, L. Jr. 1962. *Physics of Fully Ionized Gases* New York: Wiley. 2nd ed.
- Spitzer, L. Jr. 1968. *Diffuse Matter in Space*. New York: Wiley-Interscience
- Spitzer, L. Jr. 1976. *Comments Astrophys.* 6: 177–87
- Spitzer, L. Jr. 1990. *Mat.-fys. Medd.* 42(4): 157–77
- Steinholfson, R. S., Hundhausen, A. J. 1990. *J. Geophys. Res.* 95: 20,693–99
- Stone, R. G., Tsurutani, B. T. 1985. *Collisionless Shocks in the Heliosphere: A Tutorial Review*. Washington, DC: Am. Geophys. Union
- Tidman, D. A., Krall, N. A. 1971. *Shock Waves in Collisionless Plasmas*. New York: Wiley
- Tóth, G., Draine, B. T. 1993. *Ap. J.* 413. In press
- Tsurutani, B. T., Stone, R. G. 1985. *Collisionless Shocks in the Heliosphere: Reviews of Current Research*. Washington, DC: Am. Geophys. Union
- van Dishoeck, E., Blake, G. A., Draine, B. T., Lunine, J. I. 1992. In *Protostars and Planets III*, ed. E. H. Levy, J. I. Lunine, M. S. Matthews, pp. 163–241. Tucson: Univ. Ariz. Press
- Viscuso, P. J., Chernoff, D. F. 1988. *Ap. J.* 327: 364–76
- Vishniac, E. T. 1983. *Ap. J.* 274: 152–67
- Vishniac, E. T., Ryu, D. 1989. *Ap. J.* 337: 917–26
- Völk, H. J., Drury, L. O'C., McKenzie, J. F. 1984. *Astron. Astrophys.* 130: 19–28
- Wagner, A. F., Graff, M. M. 1987. *Ap. J.* 317: 423–31
- Wardle, M. 1990. *MNRAS* 246: 98–109
- Wardle, M. 1991a. *MNRAS* 250: 523–30
- Wardle, M. 1991b. *MNRAS* 251: 119–27
- Weibel, E. S. 1959. *Phys. Rev. Lett.* 2: 83–84
- Wentzel, D. G. 1974. *Annu. Rev. Astron. Astrophys.* 12: 71–96
- Wu, C. C., Kennel, C. F. 1992. *Phys. Rev. Lett.* 68: 56–59
- Zachary, A. 1987. PhD thesis. Univ. Calif., Berkeley